Coordination Chemistry Reviews 520 (2024) 216161

Contents lists available at ScienceDirect

Coordination Chemistry Reviews

journal homepage: www.elsevier.com/locate/ccr

Innovative strategies in metal-organic frameworks for enhanced electrochemiluminescence biosensors

Kai Song [a,b,*], Wei Zhao [a], Yan Zhou [c], Duo Liu [a,*], Paul K. Chu [d,**]

[a] School of Life Science, Changchun Normal University, Changchun 130033, China
[b] Research Institute for Scientific and Technological Innovation, Changchun Normal University, China
[c] State Key Laboratory of Integrated Optoelectronics, College of Electronic Science and Engineering, Jilin University, Changchun 130012, China
[d] Department of Physics, Department of Materials Science and Engineering, and Department of Biomedical Engineering, City University of Hong Kong, 999077, Hong Kong, China

ARTICLE INFO

Keywords:
Electrochemiluminescence
Metal-organic frameworks
Modification
Composite materials
Biosensors

ABSTRACT

Electrochemiluminescence (ECL) is a technique that integrates the benefits of both chemiluminescence and electrochemistry. Early illness diagnosis and hazardous material detection have both benefited greatly from its benefits, which include minimal background signal, high sensitivity, and easy operation. A novel class of porous materials known as metal-organic frameworks (MOFs) is created when organic ligands and inorganic metal nodes self-assemble. Its enormous specific surface area, many functionalized sites, adaptable structure, and range of applications in biomedicine, biosensing, and other domains have made it a hot topic in chemical and biological research. This article examines the development of MOF applications in recent years pertaining to the production of electrochemiluminescence biosensors. First, the effects of metal ions on aggregation induced electrochemiluminescence are analyzed, and design approaches for meeting the needs of ECL applications are discussed. The applications of MOFs are then categorized and described based on three factors: electroactivity, catalytically active chemicals, and carriers, in accordance with the many roles of MOFs in ECL. Lastly, present problems and obstacles are examined, and potential future routes for growth are suggested.

1. Introduction

Electrochemiluminescence (ECL) is a technique that transforms electrical energy into radiant radiation. The fundamental idea is to start with the electrode surface and produce stable precursors. From there, active intermediates are produced, which lead to high-energy electron transfer processes that build luminous excited states [1]. The electrode voltage is changed to start and regulate luminescence during the ECL process. ECL is a potent analytical technique that combines the benefits of spectroscopic and electrochemical approaches [2,3]. From this standpoint, ECL is the ideal mix of electrochemical and spectroscopic approaches, combining the high sensitivity and wide dynamic range of classical chemiluminescence (CL) with the simplicity, stability, and practicality of electrochemical methods [4]. Compared to other luminescence technologies, such as photoluminescence (PL) and CL, ECL has distinct benefits, including more exact control over the timing and location of light emission. Furthermore, ECL employs electrochemical excitation without the requirement for an excitation light source, which greatly decreases background noise to near-zero levels, whereas PL is restricted by background interference generated by non-selective light excitation [5,6]. As a result, ECL has grown in popularity in fundamental research and the identification of trace target molecules, making it an effective analytical tool.

Metal-organic frameworks (MOFs) have attracted widespread attention in the field of biosensing due to their customizable crystal structure, large specific surface area, excellent stability, and regularly adjustable pore sizes [7,8]. In recent years, researchers have designed and developed a large number of biosensors based on new MOFs and their composite materials based on different detection principles such as electrochemistry, fluorescence, electrochemiluminescence, and photoelectrochemistry to achieve high sensitivity and detection of trace amounts of target molecules and accurate detection [9,10]. The applications of MOFs in ECL sensing show a high degree of diversity. It can be used to enrich or generate high and stable ECL signals to improve the

* Corresponding authors at: School of Life Science, Changchun Normal University, Changchun 130033, China.
** Corresponding author.
E-mail addresses: songkai@ccsfu.edu.cn (K. Song), liuduo@ccsfu.edu.cn (D. Liu), paul.chu@cityu.edu.hk (P.K. Chu).

https://doi.org/10.1016/j.ccr.2024.216161
Received 14 July 2024; Received in revised form 11 August 2024; Accepted 13 August 2024

sensitivity of the sensor, and can also be used as a biosensing matrix material to assemble a variety of biomolecule recognition elements to capture more analytes. This enables MOF-based ECL biosensors to have broad prospects in the fields of clinical diagnosis, environmental monitoring, and food safety [11–13].

In this context, it is particularly important to explore the design and application of MOFs in ECL biosensors [14]. MOFs can be used as luminescent species or co-reactant carriers to improve the electrochemical activity in traditional ECL systems and achieve high-selectivity and high-affinity recognition of specific biomarkers through the introduction of specific functional groups [15]. In addition, the versatility of MOFs can further broaden the application scope of ECL biosensors through complexing with biomolecules such as nanomaterials, enzymes, and antibodies [16,17]. Previous research has focused on the design and synthesis of ECL active MOF composites [17,18], but failed to comprehensively discuss the role and design strategies of MOFs in electroactive, catalytically active substances and carrier functions in ECL.

Therefore, in this review, the design and application of MOFs in ECL biosensors are discussed in detail. First, we introduce the basic characteristics of MOFs and their mechanism of action in electrochemiluminescence, then discuss specific application examples of MOFs in improving the performance of ECL biosensors, and finally discuss the current challenges and future development directions. Through systematic research and innovative design of MOFs, it is expected to achieve faster and more accurate detection of pathogens, disease markers, and environmental pollutants and promote the development of biosensing technology to a higher level.

2. Aggregation induced electrochemiluminescence

Common ECL luminescent molecules, such as bipyridine ruthenium $Ru(bpy)_3^{2+}$ [19], lucigenin [20], peroxyoxalate [21], and luminol [22], are immobilized on electrodes via embedding, adsorption, and self-assembly methods. These sensors often suffer from issues like luminescent molecule leakage and inconsistent immobilization, leading to poor stability and reproducibility. Additionally, traditional planar luminescent molecules are prone to aggregation-caused quenching (ACQ) through π-π interactions, reducing luminescence efficiency and limiting bioanalysis applications [23–25]. Thus, developing efficient and stable luminescent materials is essential for advancing biosensing methods.

Aggregation Induced Emission (AIE) has revitalized ECL luminophore preparation by addressing ACQ issues. AIE luminophores emit weakly when isolated but show enhanced photoluminescence when aggregated [26,27]. This has applications in optoelectronic devices, stimuli-responsive materials, fluorescent probes, chemical sensing, and bioimaging [28,29]. The AIE phenomenon is based on the restricted intramolecular motion (RIM) model, which mainly includes restricted intramolecular vibration (RIV) and restricted intramolecular rotation (RIR), as shown in Fig. 1. Aggregation-Induced Electrochemiluminescence (AIECL) has emerged, where AIECL molecules exhibit higher luminescence efficiency in aggregated states due to the restriction of intramolecular motion (RIM), suppressing non-radiative transitions and enhancing ECL emission. The AIECL mechanism includes "annihilation type" and "co-reactant type" pathways [30–32].

Aggregation-Induced Electrochemiluminescence (AIECL) molecules often face challenges in achieving efficient luminescence due to complex aggregation structures, solvent effects, and intricate electrochemical reactions [29,33]. To address these issues, researchers have proposed Mediated Coordination-Induced Luminescence (MCIL) [34,35], where AIECL molecules coordinate with metal ions to form Metal-Organic Frameworks (MOFs). This coordination induces stable molecular aggregation, enhances luminescence efficiency, and optimizes electron transport pathways.

The selection of ligands and metal ions is crucial for effective MCIL [37]. Strongly coordinating ligands, luminescent functional groups, and metal ions with good electrochemical activity, such as transition metals

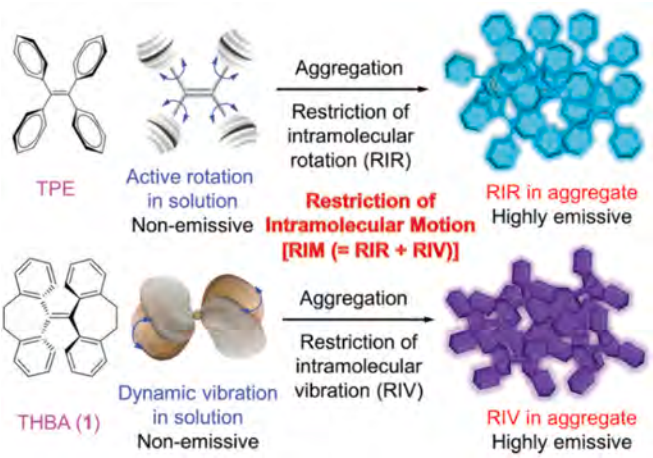

Fig. 1. RIR mechanism of AIE phenomenon (top) and RIV mechanism of AIE phenomenon (bottom) [36].

[38], rare earth metals [39], and noble metals [40], are essential. MOFs can be classified based on metal ions (e.g., single or mixed metals) [41], ligands (e.g., rigid, flexible, or functionalized) [39], and structural types (e.g., one-dimensional chains, two-dimensional layers, or three-dimensional frameworks) [42], allowing for tailored properties to meet specific application requirements. This section will discuss from the perspective of metal ion selection.

2.1. Transition metal ions

In AIECL, common transition metal ion metal organic frameworks (MOFs) include MOFs centered on zinc (Zn) [41], copper (Cu) [43], lanthanide (Ln) [44], and nickel (Ni) [45]. These metal ions induce molecular aggregation and enhance luminescence performance by forming stable coordination bonds with ligands with AIE properties. Its mechanism of action is mainly to restrict the internal rotation and vibration (RIM) of molecules, inhibit non-radiative transitions, release energy in the form of radiation, and improve the electrochemical luminescence efficiency [46]. In addition, transition metal ions also optimize the electron transfer path, reduce energy loss, and further improve the luminescence efficiency and stability of AIECL.

Lanthanide (Ln) ions have attracted much attention as luminescent probes due to their unique properties of *f-f* electronic transitions in the $[Xe]4f^n5s^25p^6$ (n = 1–14) electronic conformation [47]. These special spectral properties, including long luminescence lifetime, resistance to photobleaching, large Stokes or anti-Stokes shifts, and narrow emission bands, are suitable for analyte detection. Most biosensors are based on an "off" switch, whereas an "on" switch sensor has many advantages for many analytes [48]. The "off" probe is easily affected by the surrounding environment, such as pH, solvent, and temperature, resulting in inaccurate luminescence signals [49]. However, the analyte is coordinated and sensitized by lanthanide ions, creating an effective "on" switch that can drive the sensing system from a dark emission state to a bright emission state or adjust the emission color [50].

Gossypol is a natural toxin located in cottonseed, threatening the safety of cottonseed products. Luo et al. [51] designed a Yb-NH_2-TPDC system that, after the addition of cottonpol, produces a unique Yb^{3+} ion emission peak under light excitation, thereby sensing the cottonpol in the solution (Fig. 2 (a)). The luminescence process is attributed to the antenna effect of cottonpol on the Yb^{3+} ion, which transfers energy from the ligand to the metal ion. Liu et al. [52] designed a ratiometric fluorescence sensor based on a bifunctional iron-based metal organic framework (NH_2-MIL-101 (Fe)) to detect pesticides. NH_2-MIL-101 (Fe) can play a dual role. The 2-aminoterephthalic acid ligand gives the MOFs framework photoluminescence at 428 nm. The Fe node exhibits

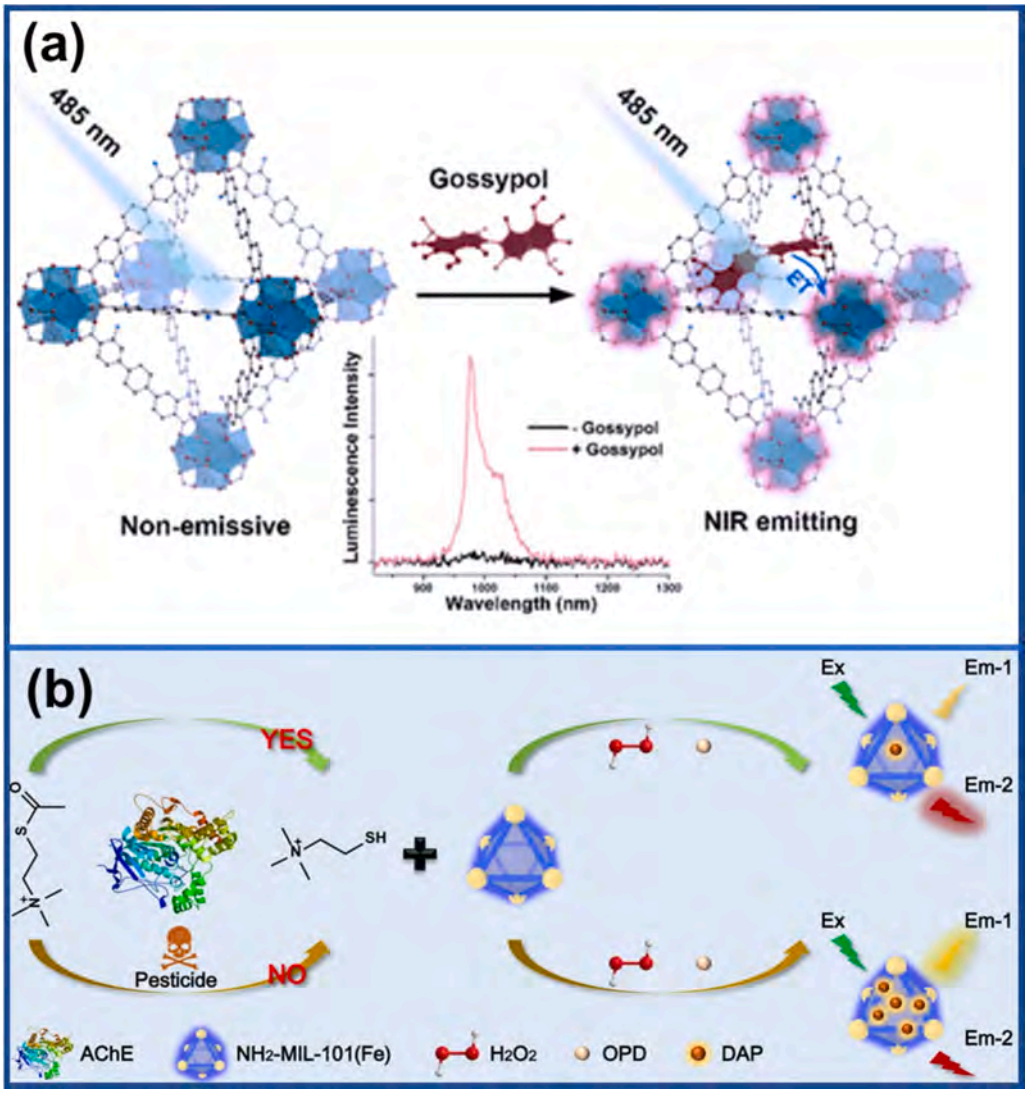

Fig. 2. (a) Schematic diagram of the Yb-NH_2-TPDC system for detecting cottonpol using the "switch" mode [51]; (b) Schematic diagram of ratiometric fluorescence sensor based on (NH_2-MIL-101 (Fe)) for detecting pesticides [52].

peroxidase catalytic activity and can oxidize *o*-phenylenediamine to diaminophenazine (DAP), emitting fluorescence at 556 nm. Due to the internal filtering effect, the intrinsic fluorescence signal (428 nm) of NH_2-MIL-101 (Fe) is suppressed (Fig. 2 (b)). When acetylcholinesterase (AChE) hydrolyzes acetylthiocholine to produce thiocholine, thiocholine has a certain reducing property and can be used to inhibit the oxidation of *o*-phenylenediamine, resulting in the inhibition of 2,3-diaminophenazine (DAP) fluorescence signal and the recovery of NH_2-MIL-101 (Fe) fluorescence. Because pesticides can effectively inhibit the activity of AChE. The presence of pesticides can increase the formation of DAP and its fluorescence signal at 556 nm, so the intrinsic fluorescence signal of NH_2-MIL-101 (Fe) at 428 nm will be suppressed again. The pesticide carbaryl has good sensitivity in the range of 2–100 ng/mL in this ratio sensor, with a detection limit of 1.45 ng/mL. For the detected target, no interference from interferents was found. The ratio sensor can be used for practical sample analysis.

2.2. Rare earth metal ions

Rare earth metal ions with europium (Eu), terbium (Tb), lanthanum (La) and gadolinium (Gd) as the center of MOFs have unique optical properties [53,54]. By forming a stable coordination complex with the AIE active ligand, it induces molecular aggregation and enhances the luminescence performance. Its mechanism of action is mainly to restrict the internal RIM, inhibit non-radiative transitions, and release energy in the form of radiation, thereby improving the electrochemical luminescence efficiency [55]. In addition, rare earth metal ions also have excellent optical stability and a long luminescence lifetime, which further improves the luminescence efficiency and application prospects of AIECL materials [56].

Dong et al. [57] designed a strategy to prepare carbon nanocomposites using an efficient and simple MOFs template(Fig. 3 (a)). Metal ions (Fe^{3+}, Zr^{4+} and La^{3+}) and 2-aminoterephthalic acid were connected by coordination bonds to form three MOFs. Then, three new MOFs derivatives were obtained by annealing at 550 °C in a N_2 atmosphere. The results of Scanning Electron Microscope (SEM) and Transmission Electron Microscope (TEM) tests showed that the three new MOFs derivatives retained the original framework of MOFs, thereby forming carbon-supported metal oxide hybrid nanomaterials. At the same time, their MOFs derivatives can be used to immobilize AChE and construct biosensors to detect methyl parathion. In particular, the wool ball-like structure of [La-MOF-NH_2]N_2, which was first reported, not only provides more active sites to increase the immobilization amount of AChE and promote electron transfer, but also shortens its diffusion length on the electrode surface. This proves the feasibility and potential value of MOFs derivatives for improving electrochemical biosensors.

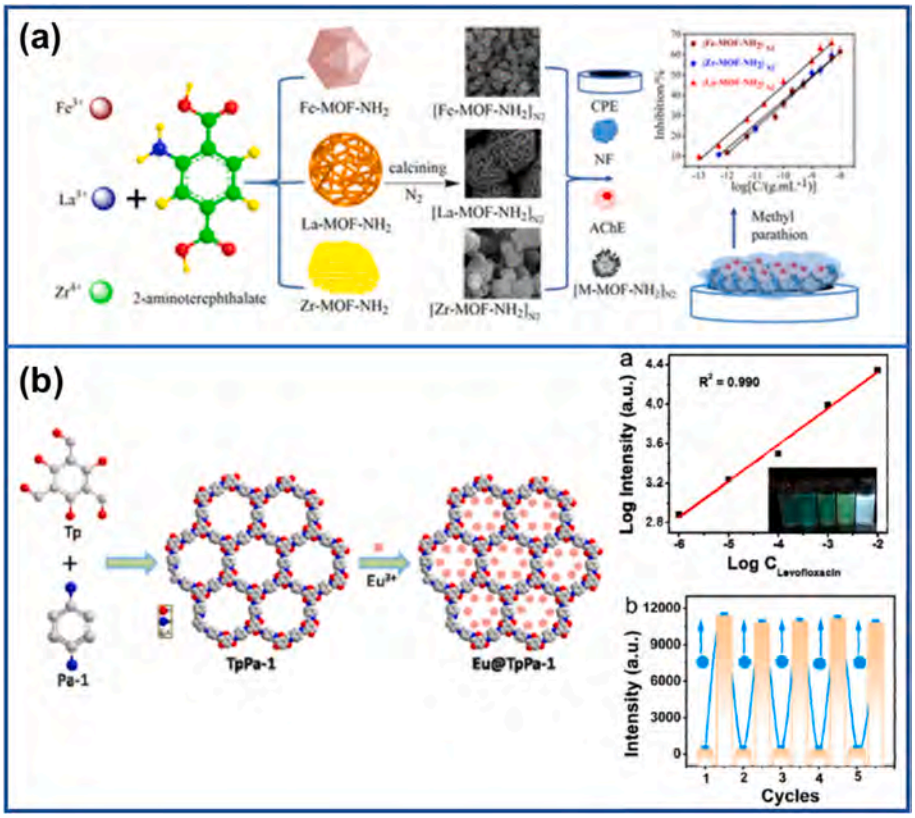

Fig. 3. (a) Schematic diagram of three new MOFs derivatives immobilizing AChE to construct biosensors for detecting methyl parathion [57]; (b) Schematic diagram of Eu@TpPa-1 as a fluorescent sensor for the detection of levofloxacin [58].

Wang et al. [58] reported another case based on an "on" switch, where they synthesized a Eu-MOF that can monitor the concentration of levofloxacin in serum and urine within one minute (Fig. 3 (b)). Wu et al. [55] used the rare mixed-valence Eu-MOF ($L_4Eu_2^{III}Eu^{II}$) to achieve stable and efficient sensitization emission of Eu^{2+} to Eu^{3+}, and further enhanced the ECL intensity by constructing CeO_2@Co_3O_4 three-layer microspheres. The near-infrared (NIR) ECL biosensor constructed based on this strategy has ultra-sensitive detection capability for CYFRA 21-1 with a detection limit of 1.70 fg/mL, which also provides a new idea for constructing efficient and non-destructive immunoassay biosensors.

Lanthanide metal ions usually exhibit strong luminescence properties after being excited due to their unique electronic structure. However, due to the forbidden nature of the *f-f* transition, its luminescence efficiency is usually low, requiring an external energy transfer mechanism to enhance the luminescence effect. This is where the antenna effect comes into play. In MOFs formed by combining lanthanide metal ions with ligands with AIE (aggregation-induced emission) properties, the improvement in luminescence performance results from the synergistic effect of the two mechanisms [59]. First, the rigid framework structure of MOFs limits the molecular motion of AIE ligands and inhibits non-radiative attenuation paths, thereby enhancing the AIE effect and significantly improving luminous efficiency [60,61].

Secondly, the antenna effect absorbs light energy through ligands and transfers it to lanthanide metal ions, effectively improving the luminescence efficiency of the ions. The enhancement of the AIE effect by the framework and the optimization of energy transfer by the antenna effect work together to significantly improve the luminescence performance of MOFs [62,63].

Due to their obvious advantages in selectivity and sensitivity, MOFs, which are porous and chemically tailorable, are ideal fluorescent sensing materials. Functional compounds can be rationally assembled into MOFs to improve the selectivity for specific analytes. On the other hand, MOFs have a high specific surface area and an adjustable internal environment, which can provide analyte adsorption/binding sites.

2.3. Noble metal ions

Noble metal ions are also commonly used to form metal organic frameworks (MOFs) and are applied in AIECL. Common types include MOFs with platinum (Pt) [64], palladium (Pd) [28], gold (Au) [65] and silver (Ag) [66] as the core. These precious metal ions are coordinated with ligands with AIE properties to form stable complexes, promote molecular aggregation and improve luminescence performance. Its main mechanism of action is to restrict the internal RIM, inhibit non-radiative transitions, and release energy through radiation, thereby improving the electrochemical luminescence efficiency [67–69]. In addition, the electrochemical stability and catalytic activity of precious metal ions optimize the electron transfer path, reduce energy loss, and further enhance the luminescence efficiency and stability of AIECL materials.

Jiang et al. [70] constructed a multifunctional enzyme catalytic biosensor by assembling nanohybrids of MOFs doped with black phosphorus quantum dots (BPQDs) and silver nanoclusters (AgNCs). The AgNCs/BPQDs/MOF nanohybrid exhibited dual emission fluorescence (FL) centers at 630 nm (red) and 535 nm (blue) under 440 nm excitation. Baicalein can enhance the catalytic activity of catalase and catalyze the decomposition of hydrogen peroxide (Fig. 4 (a)). As the content of baicalein increases, catalase accelerates the decomposition of hydrogen peroxide, and excess hydrogen peroxide is consumed. Baicalein also has the ability to inhibit the oxidation of H_2O_2. The red FL (response signal) of Ag NCs attached to MOF increases, while the blue FL (reference signal) of BPQDs doped into MOF changes negligibly. This work explored a simple and efficient semi-quantitative method for multifunctional FL visual detection, which can promote the vigorous development of biosensors. Ma et al. [71] analyzed H_2O_2 by in situ synthesizing AgNPs/Cu-TCPP nanocomposites. The results showed that

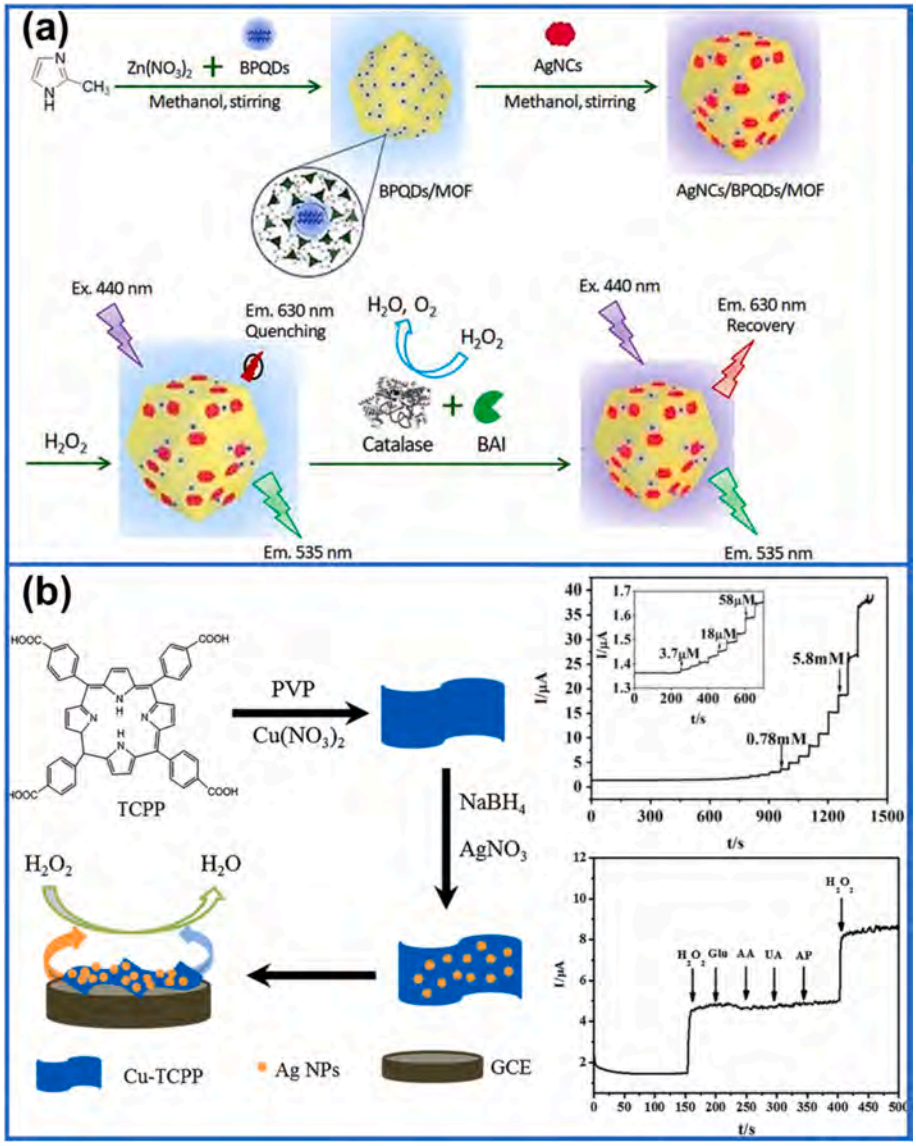

Fig. 4. (a) Schematic diagram of the detection of baicalin by AgNCs/BPQDs/MOF nanohybrids [70]; (b) Schematic diagram of the detection of H_2O_2 by Ag NPs/Cu-TCPP nanocomposites [71].

the detection limit was 1.2 μmol/L and the linear range was 3.7 to 5.8 mmol/L. Compared with previous studies, this study has the advantages of wide linear range and good selectivity (Fig. 4 (b)).

Unlike AIE molecules that form aggregates in unexpected ways through intermolecular interactions, in MOFs, AIE molecules and metals are fixed in corresponding positions through coordination bonds [72]. The position, topology and packing pattern of atoms in crystalline porous materials are all controllable [73]. Therefore, the luminescence mechanism of AIE molecules can be further understood. In addition, introducing functional AIE molecules into MOFs has unique advantages [74]:

(1) The electron transfer energy and optical properties of AIE molecules can be adjusted by adjusting nodes and ligands, including the color, wavelength, and band gap of the emitted light, to meet the requirements of practical applications [75].
(2) The network structure of metal-organic framework materials has a rigid skeleton and a special topological configuration, which can effectively limit the rotation and vibration within the molecule and avoid self-quenching, thus significantly improving the luminous efficiency [76].
(3) The porosity, open pores and adjustable internal chemical environment of the framework material can adjust the size and shape of the pores so that guest molecules fully or partially interact with AIE molecules to fix MOFs, thereby significantly improving their Sensing performance. These advantages provide a platform for designing materials with excellent luminescent properties [77].

Overall, metal-organic frameworks (MOFs) in AIECL significantly enhance the luminescence performance and stability of the sensor by coordinating with different metal ions (such as transition metals, rare earth metals, and noble metals). Transition metal ions improve the sensitivity and selectivity of the sensor, rare earth metal ions provide unique optical properties and long-life luminescence, and noble metal ions enhance catalytic activity and electrochemical stability. By further optimizing the selection of metal ions and ligands, the design of efficient, stable, and multifunctional AIECL sensors will promote their wide application in biological detection, environmental monitoring, and medical diagnosis.

3. Design strategies of MOFs in electrochemiluminescence biosensors

Metal-organic frameworks (MOFs) are organic-inorganic hybrid materials that are formed by self-assembly of organic ligands and metal ions or through coordination bonds [78]. As a solid porous material, it has the advantages of ordered porosity, ultra-high specific surface area, and adjustable structure [79]. Therefore, MOFs have attracted widespread attention in fields such as catalysis [80], gas storage [81], sensing [82], and biomedicine [83].

ECL biosensors based on MOFs have now become a research hotspot in the field of electrochemical analysis [12,84,85]. The introduction of MOFs into the construction of ECL biosensors mainly utilizes the following properties: (1) the electrochemical activity of MOFs themselves; (2) MOFs have abundant catalytic active sites, and MOFs are used as signal amplification materials to improve the sensor sensitivity; (3) Use the framework properties of MOFs to coat or encapsulate some functional components in order to achieve target performance while maintaining the material's own characteristics. MOF materials used in electrochemiluminescence (ECL) sensors should have the following characteristics to ensure sensor performance optimization and expansion of application range [86,87]:

(a) High Specific Surface Area and Porosity: MOFs possess large specific surface areas and porous structures, which provide numerous active sites and extensive contact areas. This significantly enhances the capture efficiency and sensitivity of the sensor towards target analytes. Such characteristics are crucial for amplifying the ECL signal and improving the sensor's response speed [88].
(b) Excellent Electrochemical Activity: The metal centers and organic ligands in MOFs should exhibit excellent electrochemical activity to actively participate in or promote the ECL process. MOFs containing metal centers like ruthenium and iridium, which are capable of participating in electrochemical reactions and generating ECL, are particularly suitable for such applications [15].
(c) Stability: MOFs used in ECL sensors must demonstrate robust chemical and mechanical stability, especially during repeated electrochemical cycles. Additionally, these materials should withstand various pH levels and electrolyte environments to adapt to diverse experimental and application conditions [89].
(d) Ease of Functionalization and Modification: The chemical composition and structure of MOFs should allow for easy functionalization and chemical modification. This flexibility enables the introduction of specific functional groups, such as luminophores, recognition sites, or other components that enhance the ECL effect [16].
(e) Biocompatibility: For biomedical detection, the MOFs used in ECL sensors must be biocompatible, ensuring that they do not induce toxicity or adverse effects on biological samples [90].
(f) Selectivity and Specificity: By carefully selecting different metal centers and organic ligands, MOFs can be designed to exhibit high selectivity and specificity for particular analytes. This characteristic is essential for developing highly selective sensors [91].
(g) Rapid Responsiveness: MOFs should possess a well-defined pore structure and appropriate pore size to facilitate the rapid adsorption and desorption of target analytes, thus achieving a quick response time [92].

Considering the diverse application requirements of MOFs in ECL sensors, designing and synthesizing MOFs with these characteristics can significantly enhance the overall performance of ECL sensors. Improvements in sensitivity, stability, specificity, and adaptability will play crucial roles in environmental monitoring, disease diagnosis, and food safety.

With the continuous deepening of research on MOF materials, more and more research work has begun to shift from the structural design, synthesis, and conventional performance exploration of MOF materials to the design of new functional MOFs, with targeted solutions to the bottlenecks faced by MOFs in different fields [93]. Functionalized MOF materials not only overcome their inherent defects but also further improve their performance and impart more functionalities such as optical, electrical, magnetic, and other properties. Based on the characteristics of MOFs, such as high porosity, uniformly arranged lattice structure, and adjustable pore size and shape, functional MOF materials have been widely used in drug delivery [94], electrochemical catalysis [95], gas storage [96], heavy metal ion adsorption and separation [97], biosensing [98].

According to the synthesis scheme of MOF materials and designability of the structure, functionalization of MOFs can be considered from the following aspects [99–101]: (1) Linker functionalization; (2) Metal ion functionalization; (3) Pore channel functionalization (as shown in Fig. 5(a-c)). By introducing ligands with specific functions into the framework of MOFs or introducing functional groups through post-modification methods, MOFs can be endowed with specific recognition abilities [80,102]. For example, by introducing ligands containing carboxyl, amino, or thiol groups, the affinity of MOFs for specific biomolecules can be enhanced.

3.1. Functionalization of organic ligands

During the entire construction process of MOFs, the integrity of the organic ligand structure is usually not damaged, and the inherent unique advantages and functions can be retained in MOFs. Functional groups with strong π-electron systems such as benzene, pyridine, naphthalene, and imidazole to modify organic ligands are usually prone to forming large dislocation regions, which can be monitored through UV absorption, luminescence radiation, and charge migration. Functionalized MOFs constructed with such conjugated organic ligands can more fully utilize the ligand-ligand π-π stacking strategy to promote charge delocalization and accelerate electron transport [106,107].

The first conductive MOFs (FPTRMC) with persistent porosity and high charge mobility were reported by Narayan et al. [108]. The organic ligand used in the design and synthesis of a highly conductive MOF material (Zn_2(TTFTB)) was thiafulvalene-tetrabenzoate (H_4TTFTB) functionalized with benzoic acid. Zn_2(TTFTB) achieves good conductivity by using π-π stacking between neighboring ligands in the structure as a charge transport channel. The charge mobility of Zn_2(TTFTB) is 0.2 $cm^2/V{\cdot}s$, based on the experimental results of flash photolysis-time-resolved microwave conductivity (FP-TRMC). Charge mobilities comparable to those of the finest conducting organic polymers by an order of magnitude. Thus, to increase the conductivity of MOFs, organic ligands with strong π-electron systems can rely on orbital overlap between neighboring ligands to provide additional electron transfer channels through non-covalent interactions. Based on these organic ligands, large π-conjugated system MOFs may also be employed as photosensitizers to boost MOFs' light absorption and raise the quantity of electron-hole pairs produced in the presence of sunshine, thereby increasing the MOFs' effective light capture and light contact area. Through cyclization synthesis employing pieces of hexaphenylbenzene in a prepared framework, Qin et al. [109] developed a large π-conjugated MOF material (PCN-136). According to experimental data, as seen in Fig. 6(a), the creation of large π-conjugated systems on organic linkers greatly improves the photoresponsive characteristics of MOFs. PCN-136 can decrease CO_2 under visible light irradiation, demonstrating greater activity than the system without the big π-conjugated system. This is because PCN-136 uses the metal oxo cluster as the catalytic site and the large π-conjugated system as the photosensitizer.

Functional modification of MOFs using biomolecules (DNA, enzymes, antibodies, peptides) is the basis for realizing material biosensing applications [101,110,111]. The large specific surface area and abundant pores of MOFs can provide loading sites for biomolecules, and the

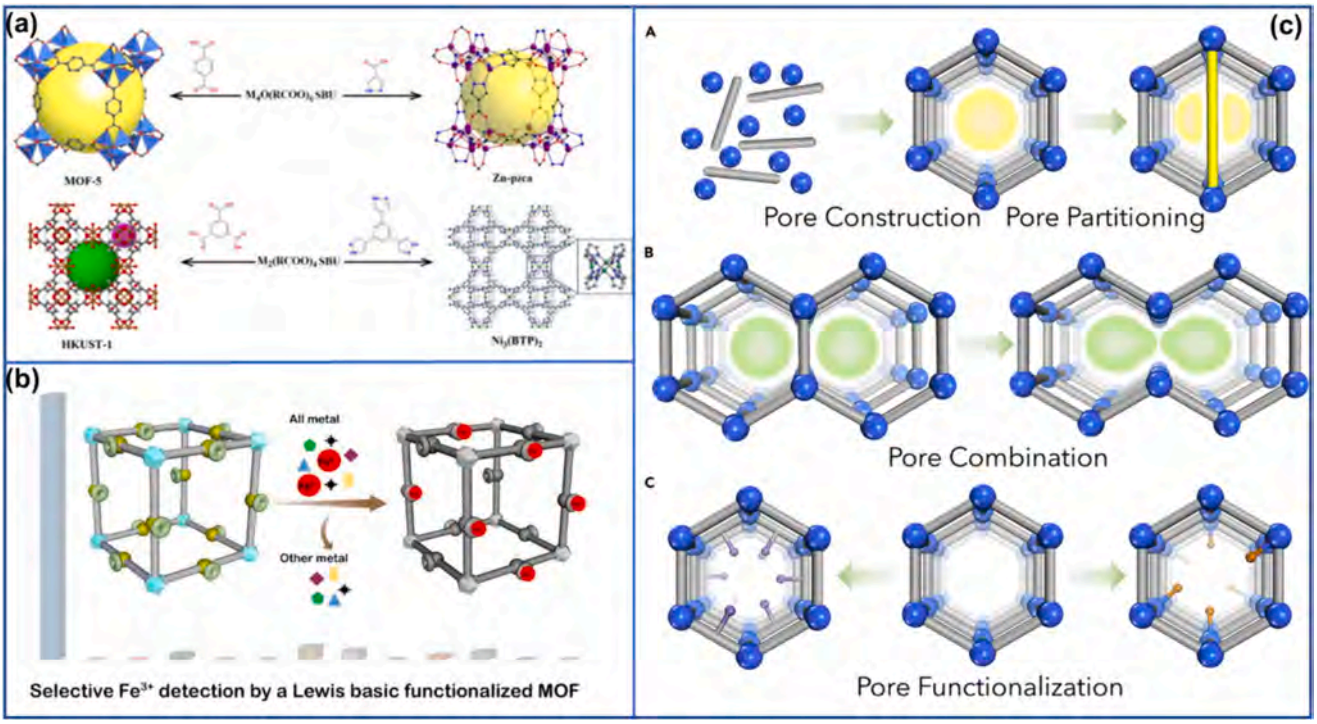

Fig. 5. Biofunctionalization methods of MOFs: (a) Linker functionalization [103]; (b) Metal ion functionalization [104]; (c) Pore channel functionalization [105].

pores of MOFs create a mild microenvironment for biomolecules, which is conducive to maintaining the activity of biomolecules. Amino-functionalized MOFs can adjust their pore environment/size while improving interactions with guest molecules. At present, there are three main ways to combine biomolecules with MOFs: physical adsorption, covalent connection, and entrapment [112,113].

MOFs functionalized with amino and carboxyl groups can also form covalent bonds with active groups on biological molecules such as DNA, proteins, peptides, and enzymes. Biomolecules are connected to MOFs through covalent coupling to expand their applications in biologically related fields [114,115]. MOF-biomolecule hybrid materials constructed through organic ligands containing amino and carboxyl groups not only have higher biological activity and biocompatibility [116]. Moreover, the targeting and selectivity of other biological molecules are enhanced, and the functional development of "1 + 1 > 2" can be achieved. By amide linking carboxyl-functionalized MOF materials and cytosine-rich nucleic acids with amino groups, Sheng et al. [117] suggested creating a responsive DNA/MOF combination. The dye rhodamine 6G may be put into DNA/MOF to provide visible drug release monitoring. At pH 5.5, cytosine-rich shows an i-motif structure resembling a cap to cover the MOF channels. The cap opens and releases rhodamine 6G from the MOF channels when the pH reaches 7.4.

In recent years, a large amount of research has been conducted on directly mixing various types of organic ligands with metal ions to construct mixed-ligand MOFs with a variety of target properties, as shown in Table 1. Lei et al. [118] synthesized two electroactive ligands, 9,10-bis(p-carboxyphenyl)-anthracene (DPA) and 1,4-diazabicyclo [2.2.2]octane (D- H_2) serve as the luminescent molecule and co-reactant in the binary electrochemiluminescence (ECL) system respectively. A kind of luminescent MOFs (m-MOF) with redox activity was designed and synthesized. ECL experiments show that the ECL emission intensity of m-MOF is 26.5 times that of the free DPA and D-H_2 mixture. This multifunctional m-MOF not only shortens the distance of the electron transfer pathway within the network structure, but also avoids the agglomeration of luminophores.

3.2. Functionalization of metal ions

The functionalization of metal ions or metal clusters is a significant method to enhance the performance of MOFs, in addition to the functionalization of organic ligands. Nearly all metal elements are included in the selected range of metal nodes in MOFs. Currently, the majority of functionalized MOFs select transition elements and lanthanide elements (Ln) as metal ion centers while building [129,130]. Since the configuration of Ln^{3+} is characterized by the gradual filling of the 4*f* orbital, from $4f_0$ (for La^{3+}) to $4f_{14}$ (for Lu^{3+}), which can produce various electronic energy levels and is insensitive to the surrounding chemical environment, narrow 4*f*-4*f* transitions are prone to occur [131]. However, the *f*-*f* transition of Ln^{3+} is a forbidden transition, and unless high-power light is used for excitation, the intrinsic luminescence efficiency of Ln^{3+} is very low. This problem can be effectively solved by using the "antenna effect". By selecting a suitable organic ligand as a sensitizer to transfer energy to Ln^{3+}, the sensitized Ln^{3+} can produce high and stable characteristic luminescence [132].

Select two or more Ln^{3+} with similar atomic radii and chemical properties, and functionalized Ln-MOFs for multi-emission can be obtained by adjusting the ratio between different Ln^{3+}. The first color-tunable intrinsic luminous MOF gel material was suggested by Chen et al. [133]. To create a full-color emitting MOF gel; the researchers chose to employ 3,5-di carboxy phenylboronic acid (5-boronoisophthalic acid) with non-uniformly distributed carboxyl groups as the organic ligand and the lanthanide ions Tb^{3+}, Eu^{3+}, and Dy^{3+} as the metal ion centers. The three inherent primary hues of red, green, and blue are represented by the light emitted by Eu-MOF (red), Tb-MOF (green), and Dy-MOF (blue) in the single-metallic MOF gel. Consequently, by varying the metal ion content, the MOF gel may provide full-color fluorescence emission when all three of these metal ions are present in the same MOF. The enormous application potential of MOFs in Light Emitting Diode (LED), multi-target detection, and other sectors is further expanded by this novel MOF gel material, which has unique optical characteristics and good viscoelasticity.

The energy of the (n-1)*d* orbital is similar to that of the ns orbital, so in addition to the lanthanide metal elements listed above, transition

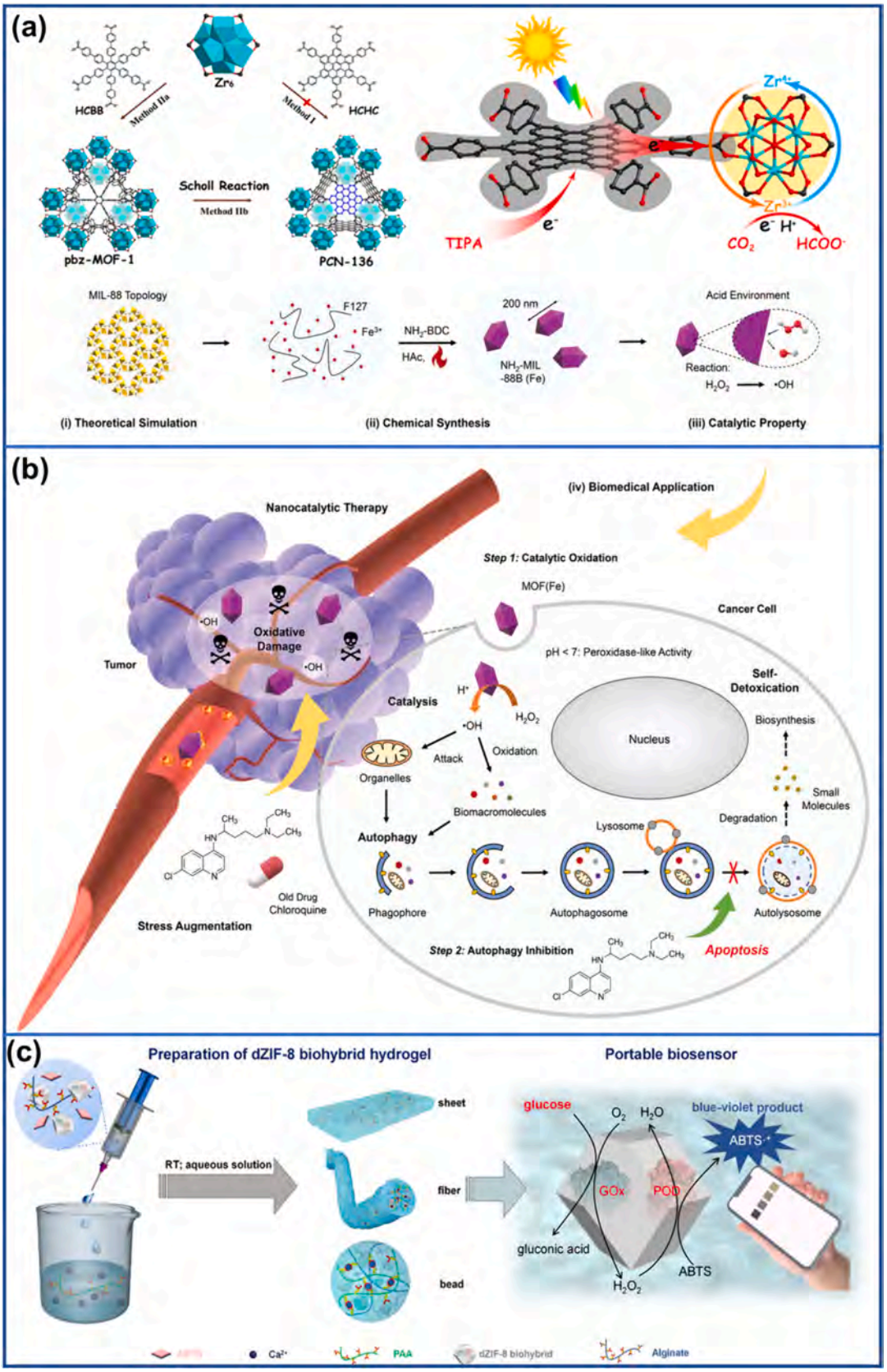

Fig. 6. (a) Large π-conjugated system as photosensitizer and metal oxo cluster as catalytic site [109]; (b) Iron-based MOF as a nanocatalyst for synergistic treatment of cancer [141]; (c) Encapsulation of enzymes into defective MOFs cavities to synthesize dZIF-8 BH gels [159].

Table 1
Mechanisms and effects of different functionalized organic ligands in the MOF structures on ECL sensors.

Functionalized organic ligands	Mechanism of action	ECL sensor effect	Refs.
Ligands with amino groups (-NH_2)	Enhance electronic supply capabilities	Improve electrochemical activity, enhance ECL luminescence intensity, and improve detection sensitivity of analytes	[119,120]
Pyridine ring-containing ligands	Provide additional coordination sites	Improve the interaction between MOFs and luminescent metal centers to improve ECL efficiency	[19,121]
Ligands containing thioether (-SR)	Increase the electron density and stabilize metal centers	Improve the stability and reusability of sensors and enhance electrochemical signals	[122,123]
Ligands containing carboxylic acid (-COOH)	Enhance the adsorption capacity of target analytes	Improved specificity and selectivity for targeting specific biomarkers	[91,124]
Fluorophore-containing ligands	Introducing internally illuminated markers	Realize dual-mode detection and increase the diversity and reliability of detection signals	[125,126]
Ligands containing phosphate group (-PO_4H_2)	Enhance coordination ability with metal ions	Improve the structural stability of MOFs and enhance the ability to capture heavy metal ions	[127,128]

metal elements (like Mn, Cu, Ni, Co, etc.) with electrons in the d orbital of the sub-outer layer also have an energy that is similar to the ns orbital. This makes it possible for many transition metal elements to have many active sites and metal valence states. Materials for MOFs made of transition metal ions are frequently employed as electrocatalysts for various electrocatalytic processes [134,135]. For the purpose of catalyzing oxygen evolution reactions (OER), Wang et al. [136] designed and built an ultra-long array and highly aligned two-dimensional Co-MOF using Co^{2+} as the metal ion center and thiophene dicarboxylic acid (H_2TDC) as the organic ligand. Compared to commercial RuO_2 catalysts, Co-MOF/NF grown on nickel foam achieves 10 and 50 mA·cm^2, respectively, at overpotentials of 270 mV and 317 mV. In order to improve the electrocatalytic OER process, Zhao et al. [137] (101) built a two-dimensional conductive nickel-cobalt bimetallic organic framework (NiCo-UMOFNs) using Ni and Co sites as catalytic active centers for OER. NiCo-UMOFNs have an ultra-thin nanosheet structure with a thickness of around 3.1 nm thanks to ultrasonic treatment. It is discovered by analyzing the crystal structure of NiCo-UMOFNs that the six O atoms coordinate the octahedral Co and Ni atoms. Unsaturated metal sites are created because the surface metal atoms do not coordinate with BDC. The occupation of coordinated unsaturated metal orbitals is optimized following the synthesis of NiCo-UMOFNs, and the strong coupling effect that forms between CoNi bimetals can further enhance the electrocatalytic activity. In contrast to RuO_2, a catalyst that is sold commercially, UMOFNs need an overpotential of 180 mV in order to achieve 10 mA·cm^{-2}.

A nickel-manganese-based bimetallic organic framework (NiMn-MOF) nanosheet was recently developed and fabricated by Cheng et al. [138] as a bifunctional oxygen electrocatalyst. To create MCCF/NiMn-MOF materials, the researchers grew electroactive NiMn-MOF nanosheets on multi-channel carbon fiber (MCCF) with excellent electrical conductivity. Based on the baseline RuO_2 electrocatalyst, oxygen reduction reaction (ORR) and OER experimental tests demonstrate that MCCF/NiMn-MOFs have superior electrocatalytic performance than commercial Pt/C electrocatalysts. The study also found that the thermodynamics of important O and OOH intermediates are effectively promoted by the significant synergistic interaction between neighboring Ni and Mn nodes in MCCF/NiMn-MOFs, speeding the kinetics of ORR and OER reactions. Theoretical calculation findings demonstrate that MCCF/NiMn-MOFs exhibit increased oxygen catalytic activity due to the successful adjustment of the 3d electronic structure of the Ni active center by the inclusion of Mn metal nodes.

In addition, selecting metal ions with high biocompatibility and endogenous content (such as Mn, Zn, Fe, etc.) can effectively reduce the toxicity of MOFs. The carriers (drugs, nucleic acids, proteins) that can be further applied in cancer therapy are used in biological transport, antibacterial agents, and biocatalysis [139,140], as shown in Table 2. To maximize oxidative damage generated by reactive oxygen species for synergistic cancer therapy, Yang et al. [141] used iron-based MOFs as nanocatalysts and employed an autophagy inhibition method, as seen in Fig. 6(b). The metal ion center Fe^{3+} in NH_2-MIL-88 exhibits enzyme-like activity in an acidic environment, making it a useful catalytic active center for the effective breakdown of H_2O_2. The enzyme-like catalytic performance of NH_2-MIL-88(Fe) was investigated using Michaelis-Menten steady-state kinetics (Michaelis-Menten), and a colorimetric technique was chosen to identify the •OH produced in the catalytic process. A Michaelis-Menten curve was produced after the absorbance of the blue product was measured at 652 nm, and the data were tracked. The findings demonstrate that the engineered NH_2-MIL-88(Fe) has a remarkably high catalytic efficiency when compared to horseradish peroxidase and can successfully catalyze the production of •OH in tumor tissue. To provide therapeutic benefits, this activity will oxidatively harm cancer cells and prevent them from proliferating further.

3.3. *Guest molecules in pores as functional active sites*

During the construction process of MOFs, the framework formed through the self-assembly of coordination bonds has a large number of intramolecular pores. The stable framework structure and adjustable pores of MOFs allow functionalization and modification of different guest molecules (gas molecules, drug molecules, bioactive molecules) to expand into more research fields [7,149], as shown in Table 3.

Luminescent guest molecules (such as organic dyes, metal ions, metal complexes, metal nanoclusters, quantum dots, and mixed peroxides, etc.) are placed in the host MOF pores to obtain functionalized MOF materials with luminescent properties [150,151]. In order to create a Rh6G@MOF composite, Chen et al. [152] introduced the fluorescent dye rhodamine 6G (Rh6G) as a guest into the primary framework of MOFs. This composite is capable of efficiently detecting hazardous contaminants and the very explosive chemical 2, 4, 6-trinitrophenol (TNP). The substance displays two emission peaks from the tpt ligand (tpt = 2, 4, 6-tris(4-pyridyl)-1, 3, 5-triazine) and Rh6G at 363 nm and 580 nm, respectively. The tpt ligand's luminescence is greatly suppressed in the presence of TNP, although Rh6G's response is hardly impacted. By monitoring the intensity ratio emanating from the two emission peaks, TNP molecules may be effectively identified.

Rhodamine B (RhB) was encapsulated into hierarchical pore Al-MOF by Gao et al. [153], who successfully used this RhB@Al-MOF material for live cell imaging of MGC-803 malignancy. It was shown by the scientists that RhB@Al-MOF could be biodistributed to various organs, with the liver, stomach, lungs, and kidneys showing the greatest concentration. This suggests that the material may enter the bloodstream and reach all tissues. The great tunability of MOFs' organic ligands may be paired with lanthanide ions added as guest molecules. This interaction can be exploited to create self-enhanced luminescence MOFs by promoting energy transfer or creating an antenna effect. An evident antenna effect and energy transfer occur between the organic ligand and Tb^{3+} in a Tb@Zn-MOF system, as described by Ji et al. [154]. In order to construct a turn-on sensor responsive to aspartate, this host-guest interaction was utilized.

In addition, by utilizing the interaction between metal ions or

Table 2
Functionalization mechanisms and effects of metal ions in different MOFs on ECL sensors.

Metal ion	MOFs types	Mechanism of action	Linear range	Limit	Refs.
Iron (Fe)	CdTe QDs@NH_2-MIL-88 (Fe)	Enhance ECL signal through redox reaction of Fe	1.0 × 10^{-6}-1.0 μg/L	0.3 pg/L	[142]
Copper (Cu)	Cu:Tb-MOF	Provide effective electron transfer channels and affect electrochemical activity	1.0 pg/mL-50 ng/mL	0.68 pg/mL	[143]
Zinc (Zn)	Zn-NGQDs	Provides a stable framework and does not directly participate in ECL reactions	1.00 × 10^{-16}–1.00 × 10^{-10} mol/L	0.03 fM	[144]
Rubidium (Ru)	$Ru(bpy)_3^{2+}$/MOF (Ru-MOF)	As the active center of ECL luminophore	5 pg/mL-5 μg/mL	1.783 pg/mL	[145]
Iridium (Ir)	Ir-ZIF-8-NH_2	Also serves as the active center of the ECL luminophore	1 fM-1 μM	0.113 fM	[146]
Palladium (Pd)	Pd@MOFs	Catalytic redox reaction	1.0–100.0 pM	0.12 pM	[147]
Platinum (Pt)	Pt NPs@MOFs	High electrocatalytic activity enhances electrochemical signals	10 pg/mL-100 ng/mL	3.61 fg/mL	[148]

Table 3
Roles of different guest molecules of MOFs in ECL sensors.

Guest molecule	MOFs	Mechanism of action	Linear range	Limit	Refs.
Ruthenium (II) complex	Ru@Ni_3(HITP)$_2$ $Ru(bpy)_3^{2+}$	As an ECL emitter, utilizing the redox activity of ruthenium	1 fM-1 nM 1.0 × 10^{-11} mol/L-1.0 × 10^{-4} mol/L(H_2S)	0.62 fM 2.5 × 10^{-12} mol/L	[163,164]
Organic dye molecules	Zn-Bp-MOFs MWCNTs/Fc-MOF	Enhance light absorption and electron transfer of the system	1 pg/mL-10 ng/mL 10 fg/mL-100 ng/mL	0.23 pg/mL 5.39 fg/mL	[165,166]
Enzyme or biomolecule	CoNi-MOF@PCN-224/Fe MoS2NF@MWCNTs	Provide biocatalytic activity and enhance the selectivity of specific biochemical reactions	10^{-4}–10^{-13} g/mL 0.5 pg/mL-100 ng/mL	0.13 pg/mL 0.3 pg/mL	[167,168]
Metal nanoparticles	Au NPs/Zn MOF AgNPs@Co/Ni-MOF	Enhance electron transfer efficiency and provide more catalytic sites	1 fM-0.1 nM 1 pg/mL-100 ng/mL	0.3 fM 0.417 pg/mL	[169,170]
Carbon nanodots or quantum dots	GDY/Ru@MOF@NCNDs-Ru CdS QDs@MOF	Provides additional electron transfer pathways and luminescence enhancement effects	0.0005 U/mL-200 U/mL 1.0 ng/mL × 10^{-4} - 10 ng/mL	0.00013 U/mL 8.5 × 10^{-5} ng/mL	[171,172]

organic ligands and residues on the surface of biologically active molecules, biological macromolecules (such as proteins, enzymes, nucleic acids, etc.) can be embedded in MOFs channels as functional active sites, which can prevent its biological functions from being inactivated by external factors such as temperature, pH, organic solvents and inhibitors [155–157]. This forms an adjustable bionic system and expands the application of MOFs in the biomedical field. Biomacromolecule proteins and glucose oxidase were employed as guests by Chen et al. [158], who successfully encapsulated them in the MOF channels using biomimetic techniques, thereby preserving the guest molecules' biological function and natural configuration. As seen in Fig. 6(c), Zhong et al. [159] created dZIF-8 biohybrid hydrogel (BH) by encasing the enzyme within the cavity of damaged MOFs and then gelating the mixture with double-cross-linked sodium alginate. Defective MOF encapsulation in dZIF-8 BH improves enzyme stability while retaining its biocatalytic activity. Colorimetric biosensing of glucose on micro-MOF hydrogels is made possible by dZIF-8 BH, which effectively transforms glucose into a blue-violet product through a biocatalytic cascade of encapsulated enzymes. This process may be combined with a smartphone. With a linear range of 0.05–4 mM, this portable biosensor can detect glucose with high precision and selectivity. Significantly, the MOF hydrogel layer creates a very hydrophilic environment that enhances the stability of the encapsulated enzyme even further. The biosensor, after 30 days at ambient temperature, retained good sensing performance.

In general, the functionalization of MOFs mainly refers to the introduction of groups with specific functions, such as photosensitive groups, catalytic active sites, or biological recognition elements, into the skeleton of MOFs through chemical modification methods. This functionalization can significantly improve the interaction between MOFs and target analytes, enhancing the selectivity and sensitivity of the sensor. During the synthesis process of MOFs, organic ligands containing specific functional groups are introduced, such as ligands with reactive groups such as carboxyl, amino, and thiol groups. These functional groups can form stable interactions with target biomolecules. Chemically modify the synthesized MOFs and introduce biological recognition elements that can specifically recognize the target molecules such as antibodies, enzymes, DNA sequences, etc.

Since the conductivity of MOFs itself is usually low, compounding them with highly conductive materials (such as conductive polymers, carbon nanomaterials, metal nanoparticles, etc.) can significantly improve the conductivity and electrochemical activity of ECL sensors [160]. MOFs and conductive materials are physically mixed to obtain composite materials with good conductivity and porous structure. MOFs are directly grown on conductive substrates through chemical or electrochemical methods to achieve tight integration of MOFs and conductive materials [161,162].

4. Applications of MOFs in ECL biosensors

In recent years, MOFs have been widely used in ECL sensors. In the ECL system, MOFs can play four important roles: (1) The central ion is directly combined with a ligand with luminescent properties to prepare a luminophore with ECL properties [10,173]; (2) The ultra-high specific surface area of MOF can be used as a carrier for luminophores and quenchers [174,175]; (3) Some MOFs have broad UV absorption and can be used as quenchers in ECL-RET [176]; (4) MOF can also serve as a co-reaction accelerator to enhance ECL signals [177,178]. The section discusses the current research status of MOFs from three aspects: electroactive, catalytically active substances, and carriers.

4.1. Applications of MOFs as electroactive materials

Electrochemically active substances refer to substances that can undergo electron transfer under an appropriate applied voltage and

have the ability to perform electrochemical oxidation-reduction reactions on the electrode surface [179]. Common electrochemically active substances include small molecule dyes (such as thionine, methylene blue, and ferrocene) and nanoparticles (such as Prussian blue), etc. [148,180]. Electroactive MOFs refer to MOFs that have redox activity and can be directly used as electrochemical signal labels. At the same time, electroactive MOFs have a large specific surface area and can also be used as nanocarriers. Therefore, using electroactive MOFs for the construction of ECL biosensors can not only increase the immobilized capacity of biomolecules, but also effectively avoid the addition of additional redox mediators, which greatly simplifies experimental steps [181,182].

A new electrochemical immunoassay for the sensitive detection of C-reactive protein (CRP) was developed by Liu et al. [183] using nanogold-modified electroactive Cu-MOF as a signal probe (Au/Cu-MOF). The produced Au/Cu-MOF combination was utilized to label antibody proteins, as indicated in Fig. 7(a), since MOFs have a lot of copper ions (Cu^{2+}) that are necessary for electrochemical signaling. Au/Cu-MOF can, therefore, be employed in the fabrication of sensors as well as a direct signal source. Initially, platinum nanoparticle-modified covalent organic frameworks (Pt-COFs) were employed as electrode materials to increase conductivity and immobilize a lot of capture antibodies. Through immunoreaction, the capture antibody-CRP-labeled antibody creates a stable "sandwich" structure in the presence of the target protein CRP. Consequently, the sensing system introduces the signal tag Au/Cu-MOF. Through immunoreaction, the capture antibody-CRP-labeled antibody creates a stable "sandwich" structure in the presence of the target protein CRP. In order to achieve sensitive detection, the signal tag Au/Cu-MOF is inserted into the sensing interface. The strength of its electrochemical signal then correlates with the concentration of CRP. Using electroactive Au/Cu-MOF as a signal label in this system eliminates the need for additional labeling procedures, simplifying, and expedition of the detection process. Cu-MOF that is electroactive was demonstrated by Hu et al. [184], who utilized the material's inherent electrochemical response as a built-in reference signal. Through ion exchange processes, target metal ions can replace the original Cu-MOF's metal centers in the presence of target ions. This allows for the quick detection of target ions and the generation of proportionate electrochemical signals under various applied potentials. This approach offers a fresh concept for creating MOF-based electrochemical signaling probes.

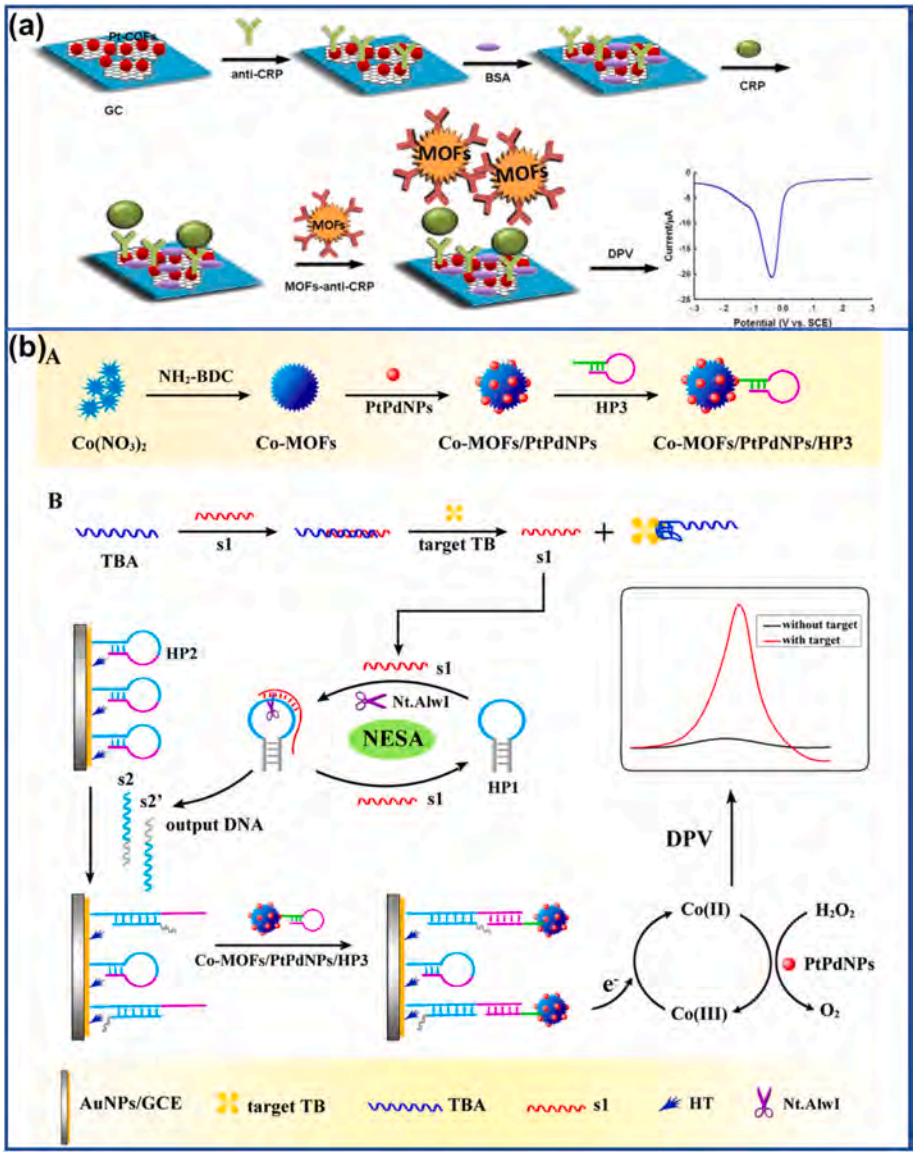

Fig. 7. (a) Schematic diagram of an electrochemical biosensor prepared using Cu-MOF as a signal tag [183]; (b) Schematic diagram of an electrochemical aptasensor constructed using Co-MOF as a signal tag [185].

In order to create a sensitive thrombin (TB) aptasensor, Yuan et al. [185] reported on an instance of electrochemically active Co-MOF and used it as a redox probe. The Co-MOF/PtPdNPs/HP3 complex was created by further modifying PtPd NPs on the surface of Co-MOF in order to trap functionalized DNA, as seen in Fig. 7(b). In order to increase the amount of S2 and S2' obtained from the circulation system and improve DNA usage, the shearing enzyme signal amplification technique (NESA) is paired with the addition of the target TB. After that, the electrode surface's capture probe HP2 is opened, exposing the unpaired base sequence and allowing HP2 to hybridize with HP3. To provide the appropriate electrochemical signal, the signal tag Co-MOF/PtPdNPs/HP3 is inserted into the electrode sensing interface. This approach eliminates the insertion of extra redox mediators by using electroactive Co-MOFs with high specific surface areas as both electrochemical signaling labels and nanocarriers. Horseradish peroxidase-like properties of Co-MOF surface-modified PtPd NPs may efficiently encourage H_2O_2 reduction and further speed up the conversion of Co^{2+} into Co^{3+} to accomplish signal amplification. With this kind of architecture, the aptasensor has strong analytical detection capabilities and provides a fresh avenue for sensor sensitivity enhancement [186].

In addition to using the central metal ions in the composition of MOFs to provide electrochemical signals, selecting ligands with redox activity to construct electroactive MOFs is also an effective strategy [187–189]. Based on the redox-active 4,4′,4″-tricarboxytriphenylamine (H3TCA) ligand and paramagnetic nickel ions (Ni^{2+}), Wu et al. [190] developed and manufactured a novel electroactive Ni-MOF. As seen in Fig. 8(a), it was employed as an electrochemical signal probe to build an electrochemical aptasensor to detect thrombin (Tb). Thrombin aptamer chains are loaded onto Ni-MOF's high specific surface area to generate the AP II bioconjugate. The electrode surface can create an AP I-Tb-AP II bioconjugate "sandwich" aptasensor by specific identification when the target Tb is present, allowing for the quantitative detection of Tb. Furthermore, Zn-MOF with exceptional electrochemical activity was prepared by Ngue et al. [191,192] by using the redox activity of the ligand 4-(1H-1,2,4-triazol-1-ylmethyl)aniline. It was employed in the sensitive detection of nitrobenzene, and more thorough discussions of the mechanism were carried out based on the molecular structure and crystal structure of Zn-MOF.

Doped Cu^{2+} as a co-reaction initiator in terbium luminous metal-organic framework (Cu:Tb-MOF) was reported by Ju et al. [143]. The formation of $SO4^{-}\bullet$ radicals during the cathodic process was boosted in the presence of $K_2S_2O_8$ co-reactant, and a highly sensitive ECL biosensor was built for the detection of gastrin-releasing peptide. The specific surface area, pore size, and ECL strength of the MOF structure are all impacted by adjusting the molar ratio and reaction time of Cu^{2+} and Tb^{3+}, which also impacts the porous and hollow shape and size of Cu:Tb-MOF. Octahedral divalent nickel coupled with terephthalic acid was used by Wei et al. [193] to create the fundamental structure of pure Ni-MOFs. The nickel hydroxide layer and terephthalic acid work together directly to create a three-dimensional skeleton. NiRu-MOFs are then created by recombining pure Ni-MOFs with the ruthenium pyridine complex. The ion exchange process disperses some of the ruthenium atoms inserted into the layer columnar structure, resulting in a notably better ECL luminous efficiency compared to pure Ni-MOFs. This work used a very effective neuron-specific enolase detection technology based on ECL immunoassay. An "ON-OFF-ON" type ECL-RET system with Ag_3PO_4-Cu-MOF as the donor and AgNPs as the acceptor was suggested by Chen et al. [194] for DES detection. A co-reactant ligand, 1, 4-diazabicyclo(2.2.2)octane, was employed by Zhuo et al. [195] together with the luminous group 1, 1, 2, 2-tetrakis(4-carboxybiphenyl)ethylene. Created orderly heterogeneous dual-ligand metal-organic frameworks (d-MOFs), which were then employed in the microRNA-141 bioassay, as seen in Fig. 8(b).

As shown in Table 4, there are still few reports on MOFs being directly employed as signaling probes in ECL biosensors and being electrochemically active themselves. Primarily because the majority of MOFs have rather unstable structures, low conductivities, and a framework that is prone to collapsing when exposed to external voltage, which somewhat restricts their utility [196,197]. Therefore, the primary focus for the design and synthesis of electroactive MOFs in the future will be on developing a straightforward and effective synthesis approach to enhance the conductive capabilities of MOFs as well as their physical and chemical properties.

4.2. Applications of MOFs as catalytically active materials

In order to meet the needs of detecting trace and ultra-trace target molecules in analytical methods, it is very necessary to establish ECL biosensors with good specificity, high sensitivity, and easy operation. In recent years, signal amplification based on nanomaterials has become one of the main means to improve the sensitivity of biosensors [202–204]. Compared with other nanomaterials, using MOFs as catalytically active materials for signal amplification has the following advantages: (1) MOFs have the advantages of abundant catalytically active sites, periodic network structure, and large specific surface area. These characteristics endow them with excellent catalytic performance [205,206]. (2) The highly crystalline configuration of MOFs gives MOFs a clear structure. This is helpful for understanding its intrinsic catalytic mechanism, thereby establishing an effective correlation between MOF's microstructural information and macroscopic electrochemical properties and providing a theoretical basis for screening MOFs with good electrocatalytic activity. This also opens up a new horizon for the development of MOFs with catalytic functions to improve the sensitivity of biosensors. The catalytic activity of this type of material generally comes from the regularly arranged metal centers in MOFs or the secondary metal structural units contained in organic ligands.

The most representative ones are the MIL series MOFs assembled from Fe(III) and polycarboxylic ligands (terephthalic acid or trimesic acid), such as MIL-53 [207,208], MIL-88 [209,210], MIL-100 [211], MIL-101 [212], etc. have been reported to have high catalytic decomposition ability of H_2O_2. In addition, MOFs based on other metal centers such as Cu, Co, and Ce have also been confirmed to exhibit outstanding catalytic properties for different test substrates. Through the catalytic premise that Fe-MOF's breakdown of H_2O_2 may efficiently enhance the oxidation of 3,3′,5,5′-tetramethylbenzidine (TMB), Wang et al. [213] ingeniously built an electrochemical sensor for lead ions (Pb^{2+}). As shown in Fig. 9(a), the current response signal is greatly improved, enabling quantitative monitoring of Pb^{2+}. An electrochemical aptasensor for the ultrasensitive detection of lipopolysaccharide (LPS) based on Ce-MOF catalytic substrate amplification was described by Shen et al. [214]. DNA hybridization was used to add functionalized HP2/AuNPs/Ce-MOF to the sensing electrode surface, as seen in Fig. 9(b). It is a very effective catalyst that enhances the electrochemical signals by promoting the oxidation reaction of ascorbic acid (AA). When combined with biological amplification technology, it achieves dual signal amplification of the entire sensing system, greatly increasing the sensitivity of LPS detection.

Certain metal-containing ligands are catalytically active in addition to MOFs with particular catalytic metal centers. Extremely catalytically active iron-based porphyrin (Fe TCPP) was employed by Ju et al. [215] as the metal node, and extremely stable zirconium element (Zr) as the bridging ligand. Based on the outstanding electrocatalytic activity of the developed porphyrin MOF (PorMOF) for the reduction of O_2, a signal-enhanced telomerase electrochemical biosensor was successfully produced, as Fig. 9(c) illustrates. The optimum activity of such MOFs and the catalytic process were further investigated by Wei et al. [216] by the use of a variety of MOFs with distinct metal nodes, namely porphyrin-coordinated metal ions. According to research findings, the catalytic activity of MOFs nearly stays the same when the core metal is switched from Zn to Co or Cu. The catalytic activity of the iron-based porphyrin ligand is greatly decreased when Fe is substituted by other metals (Zn, Co, Mn, etc.). This demonstrates that a critical factor in the catalytic

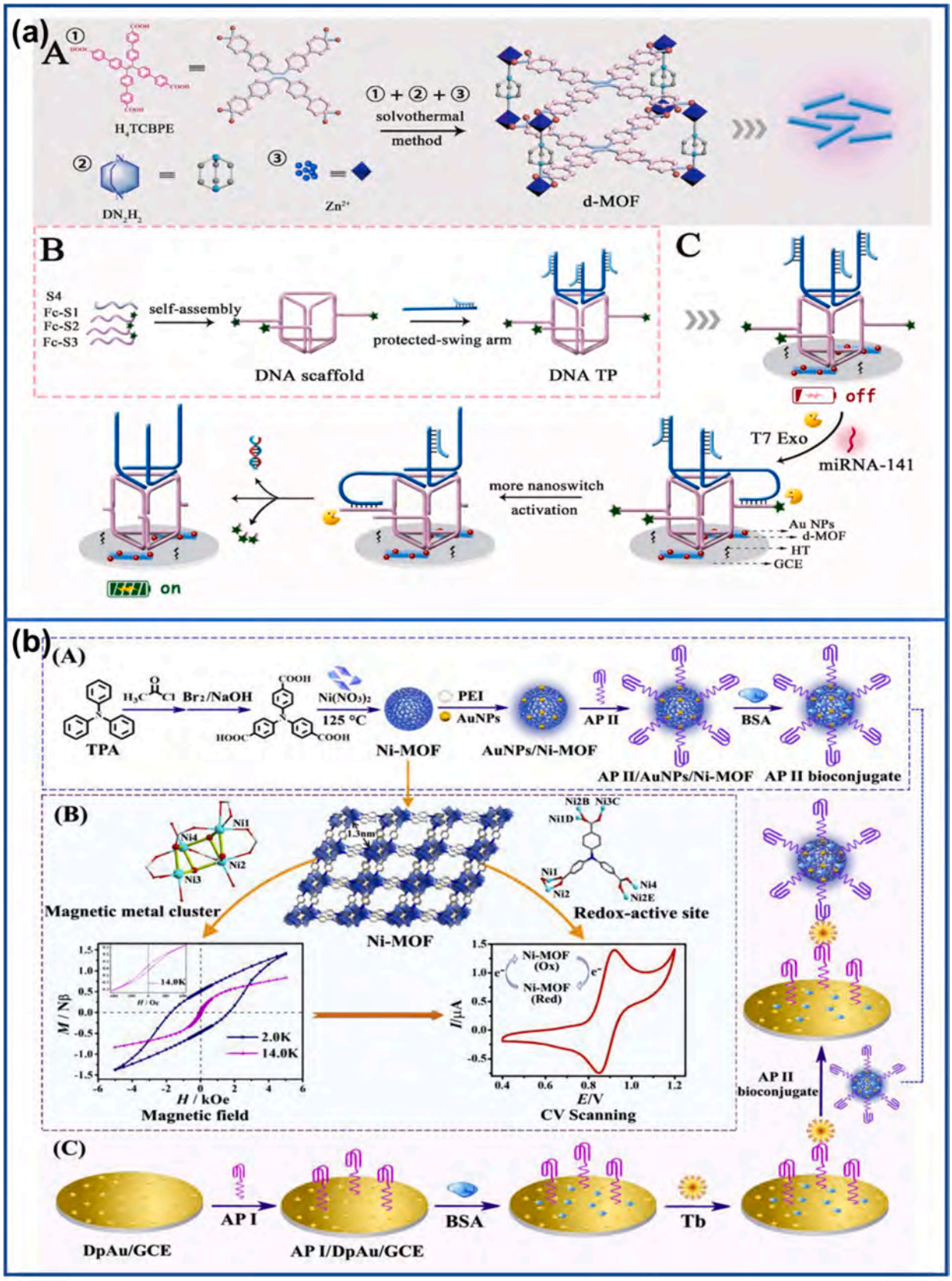

Fig. 8. (a) Schematic diagram of the electrochemical aptasensor constructed using Ni-MOF as a signal tag [190]; (b) Schematic diagram of the preparation of d-MOF and the detection process of mi RNA-141 in the biosensor [195].

Table 4
Applications of different types of MOFs as electroactive materials in ECL sensors.

MOFs types	Target analyte	ECL illuminator	Linear range	Limit	Ref
UiO-66	Cancer markers	$Ru(bpy)_3^{2+}$	5×10^{-4}–5×10^{2} U/mL	1.7705×10^{-5} U/mL	[198]
ZIF-8	Viral RNA	$Ru(bpy)_3^{2+}$	1 pg/mL-100 ng/mL	0.67 fM	[199]
MIL-53(Al)	Heavy metal ion	$Ru(bpy)_3^{2+}$	10^{-9} M–10^{-4} M	4.1×10^{-12} M (Hg^{2+})	[200]
AuNPs@Ir-Zr-MOL	Carcinoembryonic antigen (CEA)	Ir(ppy)₃	1.00 pg/mL-100 ng/mL	0.200 pg/mL	[201]
Ni-MOF	Thrombin (Tb)	H3TCA	0.05 pM-50 nM	0.016 pM	[190]

activity of MOFs is the metal center located in the catalytically active unit. Different combinations of metal centers and organic ligands can be used to create MOFs with a wide range of architectures and functionalities. When building catalytically active MOFs, this work offers a useful guide for adjusting metal centers and organic ligands selectively, which can help better control the desired features of MOFs.

As a luminous reagent carrier, Zhou et al. [217] synthesized hollow Cu/Co-MOF and loaded it with luminol. It forms an acetaminophen signal probe when it interacts with the acetaminophen complementary strand (cDNA1). Next, a malathion signal probe was created by preparing Au-g-g-C_3N_4 and loading it with the malathion complementary strand (cDNA2). A double helix structure is created by the particular recognition of aptamer and cDNA, and two signal probes are attached to the electrode that has been modified with aptamers for malathion and acetaminophen. ECL signals were created at various potentials using g-C_3N_4 and luminol. Acetamidamidine and malathion are detected simultaneously when additional pesticides are introduced because the appropriate DNA double helix structure breaks down, the signal probe slips off the electrode, and the ECL signal diminishes.

The UV–visible absorption spectra of Au@NiFe MOFs composites and ECL emission spectrum of three-dimensional $Ru(bpy)_3^{2+}$/zinc oxalate MOFs overlapped correctly, according to Wei et al. [218] It has the ability to initiate the resonance energy transfer behavior between Au@NiFe MOFs (acceptor) and $Ru(bpy)_3^{2+}$/zinc oxalate MOFs (donor). The achievement of the two-fold quenching effect on $Ru(bpy)_3^{2+}$/zinc oxalate MOFs resulted in a considerable improvement in the sensitivity of the immunosensor for Aβ42 detection. In order to encourage the reduction of dissolved O_2, Li et al. [219] utilized Au—Pd bimetallic nanocrystals and mixed-valent Ce(III, IV)-based metal-organic frameworks as co-reaction promoters. Large amounts of superoxide anion radicals (O^{2-}•) and hydroxyl radicals (OH•) are produced as a result of

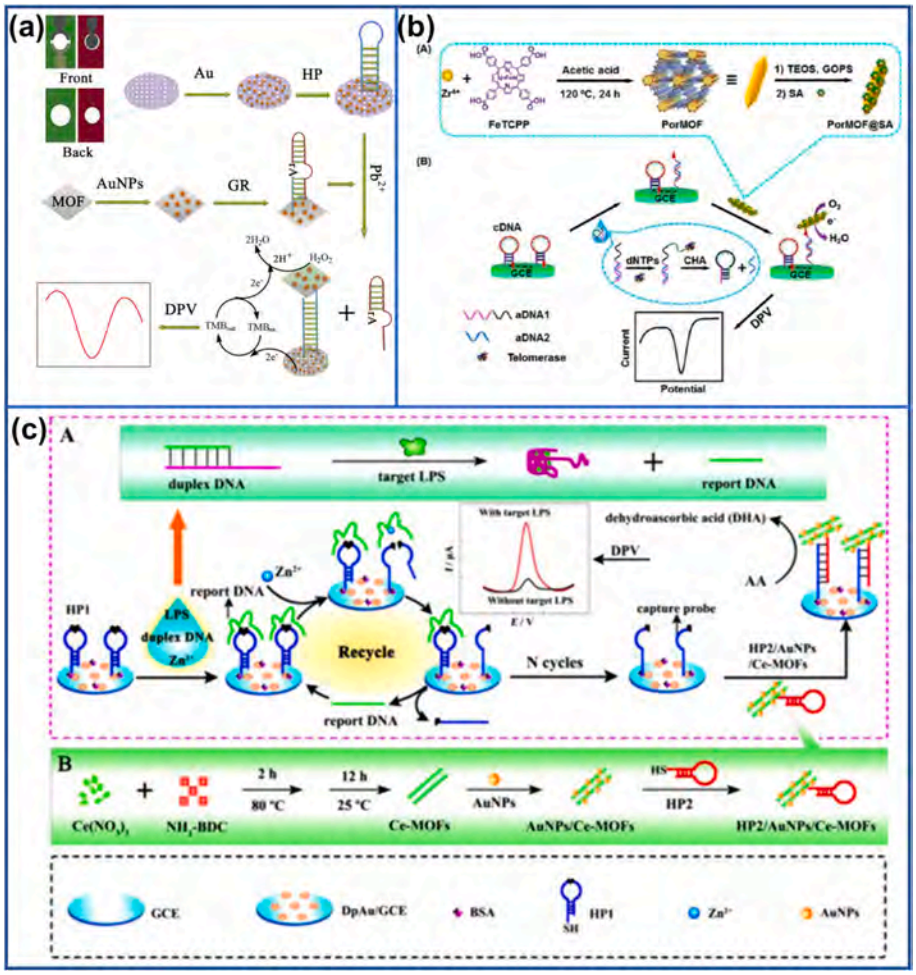

Fig. 9. (a) Schematic diagram of a Pb^{2+} electrochemical sensor constructed based on the catalytic activity of Fe-MOF [213]; (b) Schematic diagram of an electrochemical aptasensor constructed based on the catalytic activity of Ce-MOF for sensitive detection of LPS [214]; (c) Schematic diagram of preparing a signal-enhanced telomerase electrochemical biosensor based on the catalytic activity of PorMOF [215].

the cooperative catalysis of Au and Pd, the spontaneous cycle reaction of Ce(III)/Ce(IV), and the high electrochemically active surface area of Ce (III, IV) MOF. As seen in Fig. 10(a), a signal amplification ECL sensor chip was ready for sensitive procalcitonin measurement.

The above-mentioned catalytically active MOFs can effectively promote substrate decomposition and accelerate the charge transfer and redox reaction process of the electron mediator, thereby enhancing the electrochemical signal response to improve the sensitivity of the biosensor. However, the catalytic activity of most MOFs relies on the addition of substrates [220,221]. Common substrates such as H_2O_2 are unstable and easy to decompose, thus causing inevitable detection errors and complicating the entire operating system. These factors are critical for the design of biosensors. and application brings certain limitations, as shown in Table 5. In order to break the inherent defects of catalytic substrates, Yu et al. [222] synthesized a new substrate-free Ce(III, IV)-MOF electrocatalyst by adjusting the valence state of the central metal of MOFs. As shown in Fig. 10(b), Ce^{3+} in Ce(III)-MOF is partially oxidized to Ce^{4+} to obtain mixed valence Ce(III, IV)-MOF. Due to the two valences of Ce(III) and Ce(IV) Spontaneous recycling can occur between states, so the electrochemical catalysis of the small molecule thionine (Thi), which is an electrical signal, can be directly achieved without a catalytic substrate. Based on this, the authors combined DNA signal amplification technology to construct a highly sensitive thrombin electrochemical aptasensor. This study proposes the influence of the central metal valence state of MOFs on their catalytic activity and prepares multivalent metal MOFs through controlled synthesis strategies, which points out a new direction for the development of substrate-free MOF electrocatalysts for use in ECL biosensors.

4.3. Applications of MOFs as carriers

In addition to providing catalytically active sites, MOFs also become ideal solid templates due to their large specific surface area, controllable pore structure, and diverse chemical functional groups. To load a variety of guest molecules such as natural enzymes, electrochemically active substances or nanoparticles (such as precious metals, quantum dots, or metal oxides), etc. [227,228]. Utilizing the framework properties of MOFs for functional modification will become an important strategy in materials design. This not only allows the introduction of other functional components while maintaining the properties of MOFs, but also

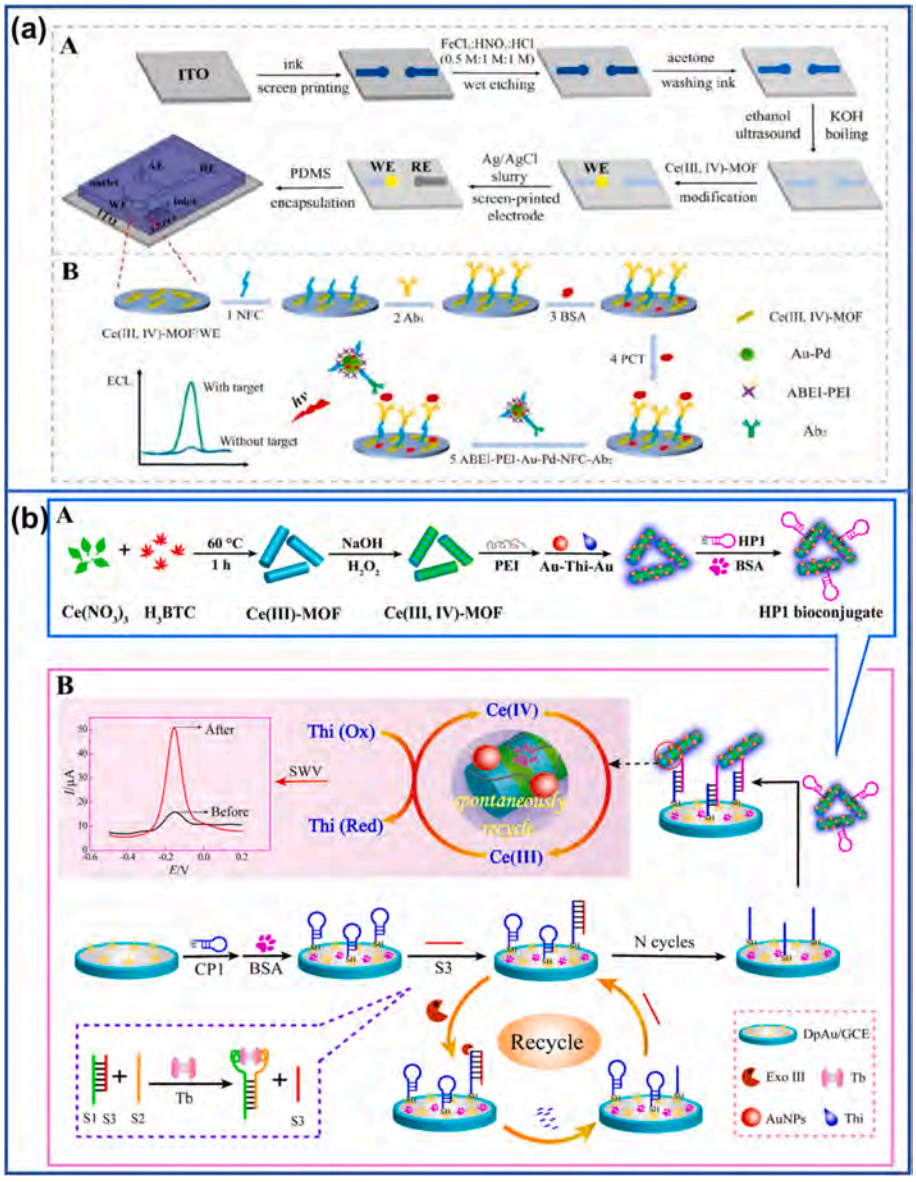

Fig. 10. (a) Schematic diagram of the construction process of the microfluidic chip and sensing platform [219]; (b) Schematic diagram of the thrombin electrochemical aptasensor constructed based on the catalytic activity of mixed valence Ce(III, IV)-MOF [222].

Table 5
Applications of different types of MOFs as catalytically active materials in ECL sensors.

MOFs types	Target analyte	ECL illuminator	Catalytic performance description	Linear range	Limit	Refs.
SPAN/HKUST-1@Luminol	H_2O_2	Luminol	Catalytic decomposition of H_2O_2 produces more free radicals	3×10^{-11}–6×10^{-10} (alkaline), 1.0×10^{-7}–3×10^{-5} (neutral)	2.5×10^{-11} (alkaline), 6.0×10^{-8} (neutral)	[223]
Ru@MOF/GCE	Antibiotic	$Ru(bpy)_3^{2+}$	Catalyze the reaction between antibiotics and ECL luminophores	30 pM-300 μM	13.7 pM	[224]
Cu-MOF	Glucose	Luminol	Enhance signal by catalyzing oxidation of glucose	6.0×10^{-7}–2.0×10^{-5} M	6.736×10^{-8}	[225]
$Ru(bpy)_3^{2+}$–UiO66 MOF	Heavy metal ion	$Ru(bpy)_3^{2+}$	Reacts with heavy metal ions to form stable complexes to enhance ECL signals	1.0×10^{-6}–1.0×10^{2} μM	1.0×10^{-7} μM	[226]
Cu/Co-MOF	Acetamiprid and malathion	Luminol	Catalytically decomposes nitrates to produce nitrogen oxides to promote ECL reactions	0.1 μM-0.1 pM	0.015 pM; 0.018 pM	[217]

benefits from the synergistic effect between MOFs and guest molecules, providing more binding sites. This will help improve the analytical performance of the sensor [229].

4.3.1. MOFs for encapsulation of natural enzymes

It is well known that natural enzymes have high catalytic efficiency, but their inherent defects, such as instability, easy degradation, and inactivation, limit wider application to sensors. Using the multi-dimensional framework structure of MOFs to encapsulate natural enzymes can protect them from biological, thermal, or chemical degradation while ensuring that the enzyme activity is not destroyed [230]. Thereby effectively improving the enzyme utilization, which also directly affects the accuracy and sensitivity of the sensor.

The co-precipitation approach was employed by Wang et al. [231] to effectively encapsulate both glucose oxidase (GOx) and NiPd nanoparticles concurrently into a zeolitic imidazolate framework (ZIF-8). Additionally, high catalytic activity GOx@ZIF-8(NiPd) was employed for the electrochemical detection of glucose. As seen in Fig. 11(a), the composite retains the enzymatic activity of GOx in addition to having the peroxidase-like activity of NiPd because the macroporous structure of ZIF-8 can coat enzymes and nanoparticles efficiently. By using this method, the contact distance between the catalytic site and the intermediate product of the cascade reaction, H_2O_2, is greatly reduced, and multi-enzyme cascade catalysis is skillfully achieved. As a result, the system shows improved catalytic stability, increased catalytic efficiency, and a quicker catalytic effect.

By selecting MOFs (PCN-888) with three distinct types of cavities, Zhou et al. [232] methodically investigated how different hole diameters might accommodate the enzymes horseradish peroxidase (HRP) and glucose oxidase (GOx). It was established that the two enzymes could only be coupled by gradually encasing them in a certain sequence. Studies also showed that PCN-888 prevented trypsin from breaking down the encapsulated enzymes while preserving the catalytic activity of both enzymes. As seen in Fig. 11(b), this demonstrates the system's

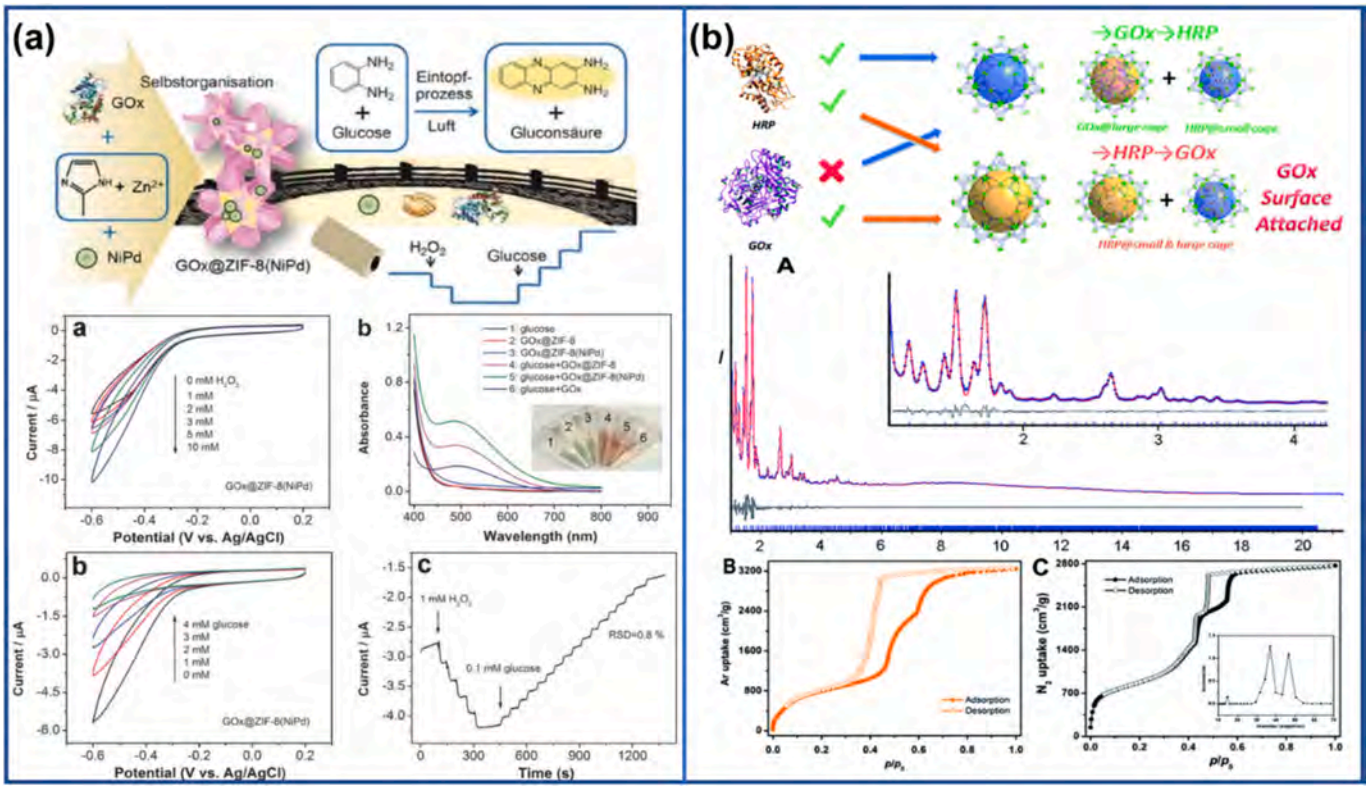

Fig. 11. (a) Schematic diagram of GOx@ZIF-8(NiPd) prepared by co-precipitation method and used for electrochemical detection of glucose [231]; (b) Schematic diagram of PCN-888 used to gradually encapsulate GOx and HRP [232].

excellent stability in both vitro and in vivo settings. The strategy of encasing biological enzymes with MOFs is strengthened theoretically by this research work, and it also offers fresh ideas for the development of sensor designs based on enzyme@MOFs composite materials as well as application to complicated biological systems.

4.3.2. MOFs for immobilization of electroactive substances

The effective immobilization of electroactive substances is a key factor affecting the signal response of ECL biosensors. Using the large surface area and flexible pore structure of MOFs to load electroactive substances can not only increase the loading capacity of electroactive substances, but also greatly shorten the distance between MOFs and signal molecules, which will help improve sensor sensitivity [55,233]. Secondly, coating signaling molecules and secondary modification of the surface of MOFs can also be used, which is also an effective strategy for designing responsive switching sensors [234]. Chang et al. [235] proposed a one-step synthesis method to coat the electroactive molecule methylene blue (MB) in the zeolite imidazole framework ZIF-90 to obtain MB@ZIF-90 with high loading capacity and good stability. Based on this, a responsive biosensor was designed for effective detection of adenosine triphosphate. In addition, Bao et al. [236] encapsulated MB into porous structure zirconium-based MOFs, and the synthesized MB@DNA/MOFs can not only be used for signal amplification, but also serve as an effective biosensing platform. A label-free and stimulus-responsive electrochemical biosensing platform based on this design was used for the sensitive determination of carcinoembryonic antigen (CEA). As shown in Fig. 12(a), in the presence of CEA, a large amount of S1 and S2 was obtained by combining biological DNA cycle amplification technology. This, in turn, leads to the exposure of surface pores of MB@DNA/MOFs, releasing the electroactive molecule MB and testing its electrochemical response.

4.3.3. MOFs for immobilization of nanoparticles

In addition to encapsulating enzymes or electroactive substances, MOFs are often used as templates to load nanoparticles, which can not only effectively avoid the decrease in activity caused by the agglomeration of small-sized nanoparticles themselves. Moreover, thanks to the interaction between host and guest molecules, it is expected to achieve the purpose of synergistic catalysis between components [237,238]. Common nanoparticles include precious metals, quantum dots, and metal oxides. To create the Pd/NH_2-ZIF-67 nanocomposite, Dai et al. [239] loaded palladium nanoparticles (PdNPs) into the zeolite imidazolate framework ZIF-67. Because ZIF-67 has a higher specific surface area than the others, it can expose more active sites and act as a catalyst to encourage Pd NPs to break down H_2O_2 in addition to acting as a carrier for Pd NPs. This design deftly enables signal amplification of the sensing system, greatly increasing the sensitivity of the sensor by making use of the synergy between ZIF-67 and PdNPs. Carbon quantum dots (CDs) were implanted in the ZrHf-MOF framework structure by Gu et al. [240], who also created a CDs@ZrHf-MOF composite with strong electrochemical activity. The electrochemical aptasensor that was built was utilized for the sensitive detection of human epidermal growth factor receptor 2 (HER-2) utilizing CDs@ZrHf-MOF as a sensing platform, as illustrated in Fig. 12(b). When ZrHf-MOF and CDs work together, they have a synergistic impact that can do more than just amplify electrochemical signals. Additionally, it can strengthen the G-quadruplex that forms between HER2 and the aptamer chain, improving selectivity and stability for the sensor.

In addition, Yu et al. [241] produced PtNi@MIL-101(Fe) with excellent catalytic performance by encapsulating bimetallic PtNi nanoclusters in MIL-101(Fe) with electrocatalytic activity used for the development of transcription factor (TF) ECL biosensors. Small-sized PtNi nanoclusters are contained in the homogeneous cavities of MIL-101(Fe), as seen in Fig. 12(c). This effectively prevents PtNi from aggregating and preserves the catalytic activity of PtNi nanoclusters. It is noteworthy that MIL-101(Fe) exhibits catalytic activity towards methylene blue (MB) on its own, hence taking advantage of the synergistic catalytic effect. PtNi@MIL-101 has superior catalytic activity for MB, leading to signal amplification and a notable increase in the sensor's sensitivity.

To create an immunosensor for the tumor marker alpha-fetoprotein, Cui et al. [242] utilized MOF-5 as a carrier to encapsulate CdS quantum

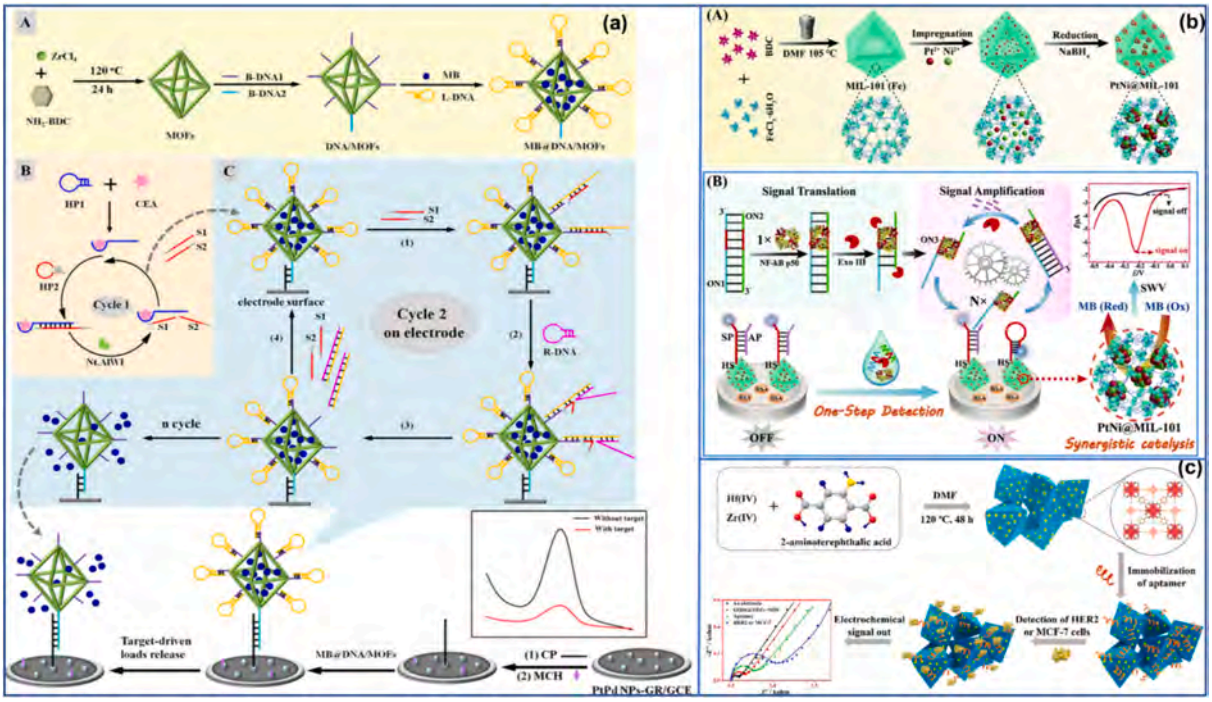

Fig. 12. (a) Schematic diagram of MB@DNA/MOFs used to design responsive ECL biosensors [236]; (b) Schematic diagram of CDs@ZrHf-MOF used as a sensing platform to construct HER-2 electrochemical aptasensors [240]; (c) Schematic diagram of TFs electrochemical biosensor constructed based on the efficient catalytic activity of PtNi@MIL-101(Fe) [241].

dots (CdS QDs) in MOF-5 as a carrier for AgNPs functionalized luminol. Co/Ni-MOF's nanosheet microflower-like assembly structure, resistance to particle agglomeration, and strong catalytic activity significantly enhance the luminol-AgNPs system's ECL performance. To catalyze the ECL reaction of luminol and H_2O_2, atomically distributed cobalt and nickel ions are packed onto ultrathin Co/Ni-MOF.

Various types of MOF materials show a high degree of diversity in ECL sensing applications [173,243]. It can be used to enrich or generate a high and stable ECL signal to improve the sensitivity of the sensor. It can also be used as a biosensing matrix material to assemble rich biomolecule recognition elements to capture more analytes, as shown in Table 6.

5. Summary and outlook

5.1. Summary

The application of metal-organic framework materials (MOFs) in the field of electrochemical biosensing has recently garnered significant attention. MOFs exhibit great potential not only as electrode modification materials, but as nanocarriers and signal probes as well. This review summarizes the application progress of MOFs in the construction of ECL biosensors in recent years. By combining the advantages of electrochemistry and chemiluminescence, ECL technology shows great potential in early diagnosis of diseases and detection of harmful substances. As a new type of porous material, MOFs are widely used in biomedicine and biosensing fields due to their customizable structure, diverse functions, large specific surface area and abundant functionalized sites. In this article, we reviewed the biosensing mechanism of ECL and explored the design strategy for ECL application needs. Subsequently, according to the different functions of MOFs in ECL, their applications were classified and summarized from three aspects: electroactivity, catalytic active substances and as carriers. Although MOFs have shown many advantages in ECL biosensors, this research field still faces challenges such as structural stability, synthesis complexity and feasibility in practical applications. Future research should focus on optimizing the structure and functionalization of MOFs, simplifying the synthesis method, and improving its application effect in complex samples. Through continuous innovation and development, the application prospects of MOFs in ECL biosensors will be broader, providing more efficient and sensitive solutions for fields such as early disease diagnosis and environmental monitoring(as illustrated in Fig. 13).

5.2. Outlook

However, MOFs still face certain limitations. For instance, their ability to identify targets is constrained, complicating signal amplification and output. Additionally, the utilization of MOF metal centers remains relatively straightforward. These critical issues hinder the further application of MOFs in electrochemical biosensing. To address these challenges, integrating nanomaterials into MOF structures can enhance conductivity. Organic or inorganic templates can guide the formation of MOF pore structures, which are retained by removing the templates post-synthesis. By adjusting synthesis conditions such as temperature, solvent, and the type or ratio of metal ions and organic ligands, the pore size and distribution of MOFs can be controlled. Optimizing pore structures can facilitate efficient molecular screening, thereby improving sensor selectivity for specific analytes.

Moreover, MOFs can be functionalized with various DNA nanostructures and signaling molecules to impart molecular recognition capabilities and signal output functions, thereby broadening their applications in biosensing. ECL, which excites luminescent species through electrochemical reactions, can be enhanced by incorporating ECL-active species into MOFs. This can be achieved by chemically bonding or physically adsorbing ECL emitters (such as quantum dots or $Ru(bpy)_3^{2+}$) onto MOFs, significantly improving ECL efficiency. Synthesizing nano-MOFs with uniform structures to increase the active area of the sensing interface will be an effective way to obtain sensors with high sensitivity and accuracy. However, since the synthesis of MOFs is self-assembled under closed conditions, the synthesis process is difficult to control and monitor in real time, so it is still a great challenge to accurately control the structure of MOFs. With the continuous exploration of nanomaterial synthesis schemes, it is expected that precise synthesis of MOFs can be achieved through optimization of synthesis methods and the assistance of additives in synthesis.

The non-covalent binding of probes to MOFs has non-specific shedding, and although there are many covalent binding methods for probes to MOFs, none of them can ensure the effective binding of probes to specific sites on MOFs. In addition, electrostatic adsorption between probes and MOFs will also interfere with covalent binding. Therefore, to achieve accurate and effective binding of probes to MOFs, it is necessary to systematically study the introduced modification groups, functionalization methods, and probe ratios of each MOFs to ensure the reproducibility and accuracy of the test results.

Constructing biosensors with MOF composite materials can extend the linear range of detection and lower detection limits. Combining multiple functional materials with MOFs can leverage the unique properties of each material. Despite the promising applications of MOF composites in biosensors, challenges such as relatively weak anti-interference ability and difficulties in high-throughput detection persist. To further enhance the performance, efforts should focus on improving the acid and alkali resistance of MOF composites, scientifically designing MOF pore sizes, and integrating technologies like microarrays and microfluidics. Biocompatibility of MOFs. When MOFs are used in biomedical applications such as in vivo detection, heavy metals contained in their structure may cause biological toxicity due to their accumulation in the body. Therefore, the development of more water-stable, low-toxic MOFs with potential clinical application value for biosensing is also an urgent problem to be solved. The toxicity and biocompatibility of MOFs are jointly determined by the metal nodes and organic ligands of MOFs, the concentration of MOFs, and the physicochemical properties of MOFs (such as hydrophobicity, particle size, etc.). By optimizing these influencing factors, MOFs with ideal performance will be obtained, which can be better applied in the biomedical field.

Other organic framework compounds, such as covalent organic

Table 6
Applications of different types of MOFs as carriers in ECL biosensors.

MOFs carriers	Target analyte	Biometric components	Linear range	Limit	Refs.
ZIF-8	DNA	Nucleic acid probe	20 pM-1 nM	18 pM	[244]
Cu-MOF	Protein	Carcinoembryonic antigen (CEA) prostate-specific antigen (PSA)	0.001–1.0 0.0001–0.05 ng/mL	0.8 pg/mL 64.5 fg/mL	[245]
Ag/Fe-MOFs	Carbohydrates (α2,6-sial-Gs)	Lectin	1 fg/mL-1 ng/mL	0.09 fg/mL	[246]
Zr-MOF	Glioblastoma (GBM)	Antibody	9.5×10^3–1.9×10^7 particles/μL	7.83×10^3 particles/μL	[247]
MOF-808	Methicillin-resistant *Staphylococcus aureus*	Biorecognition protein	10^2–10^7 CFU/mL	47 CFU/mL	[248]

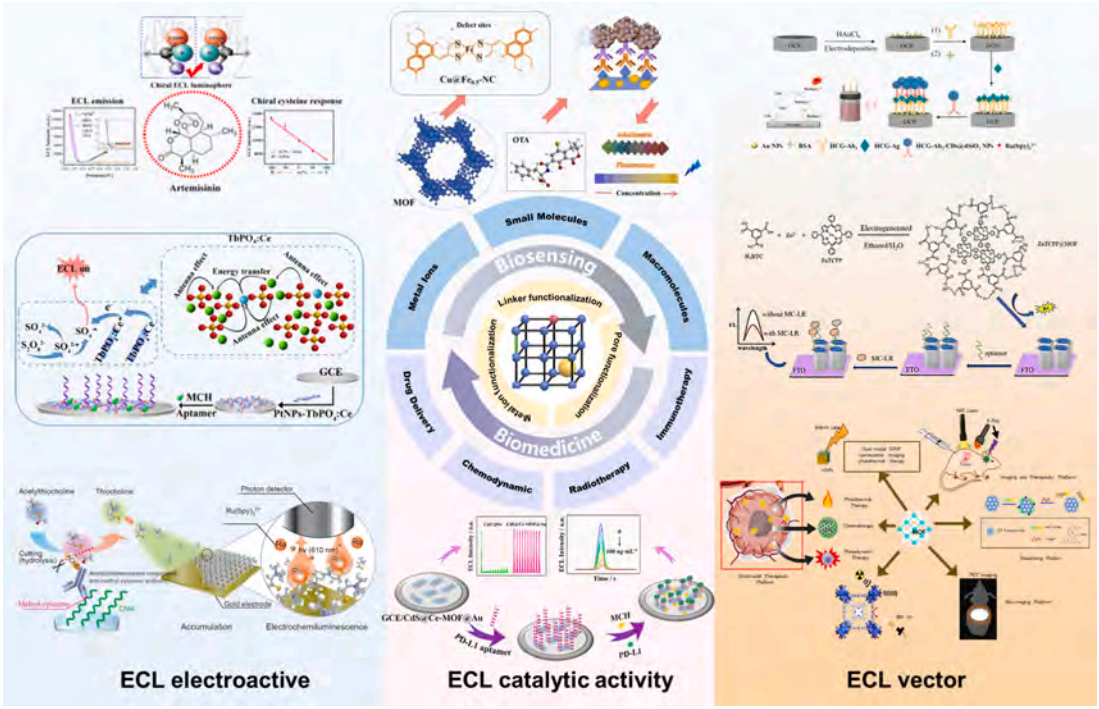

Fig. 13. Design strategy and application of MOFs in electrochemiluminescence biosensors.

frameworks (COFs) [249,250], Schiff-based organic frameworks (SOFs) [251], and hydrogen-bonded organic frameworks (HOFs) [252], have also made significant progress in their applications in electrochemiluminescence (ECL). COF has been widely used in the construction of ECL sensors due to its highly ordered pore structure, high specific surface area, and tunable electronic properties. These properties enable COF to exhibit high sensitivity and selectivity in detecting small molecules, heavy metal ions, and biomolecules [253]. The unique structure of SOF makes it an ideal choice for high-efficiency ECL materials due to its excellent electrochemical and optical properties [254]. Its synthesis is relatively simple and has good stability in solution. Due to its easy assembly and dissociation properties, HOF has gradually attracted the attention of researchers and been applied in ECL systems [255]. However, the application of these framework materials in ECL still faces some challenges. The first is the issue of structural stability, especially when it is prone to degradation during long-term electrochemical cycles. Secondly, the complexity and controllability of the synthesis process still need to be improved. In addition, the reproducibility of the performance of these materials in aqueous solutions and the feasibility of practical applications are also important issues that need to be addressed. Through further structural optimization, synthesis method improvement and application exploration, the application prospects of these framework organic compounds in the field of ECL will be broader.

On the heels of the continuous discovery of new materials and advancements in artificial intelligence and 3D printing technology, biosensors based on MOF composite materials are expected to evolve towards miniaturization, integration, multifunctionality, intelligence, and ultra-low power consumption. These sensors are anticipated to play increasingly significant roles in clinical diagnostics, biosafety, food safety, and environmental monitoring.

Funding

This work was supported by Independent Innovation Capacity Project of Jilin Province Functional Biomolecular Engineering Research Center (2023C020).

Declaration of competing interest

The authors declare that they have no known competing financial interests or personal relationships that could have appeared to influence the work reported in this paper.

Data availability

No data was used for the research described in the article.

Acknowledgments

We thank Home for Researchers editorial team (www.home-for-researchers.com) for language editing service.

References

[1] Y. Zhao, L. Bouffier, G. Xu, G. Loget, N. Sojic, Chem. Sci. 13 (2022) 2528–2550.
[2] A. Zanut, A. Fiorani, S. Canola, T. Saito, N. Ziebart, S. Rapino, S. Rebeccani, A. Barbon, T. Irie, H.-P. Josel, Nat. Commun. 11 (2020) 2668.
[3] Y. Liu, H. Zhang, B. Li, J. Liu, D. Jiang, B. Liu, N. Sojic, J. Am. Chem. Soc. 143 (2021) 17910–17914.
[4] H. Nasrollahpour, B. Khalilzadeh, A. Naseri, M. Sillanpaa, C.H. Chia, Anal. Chem. 94 (2021) 349–365.
[5] Y. Zhao, J. Descamps, N. Al Hoda Al Bast, M. Duque, J. Esteve, B. Sepulveda, G. Loget, N. Sojic, J. Am. Chem. Soc. 145 (2023) 17420–17426.
[6] M. Hesari, Z. Ding, Nat. Protoc. 16 (2021) 2109–2130.
[7] Y. Zhao, H. Zeng, X.-W. Zhu, W. Lu, D. Li, Chem. Soc. Rev. 50 (2021) 4484–4513.
[8] J.E.D.S. Souza, G.P.D. Oliveira, J.Y. Alexandre, J.G. Neto, M.B. Sales, P.G.D. S. Junior, A.L.D. Oliveira, M.C.D. Souza, J.C.D. Santos, Electrochem 3 (2022) 89–113.
[9] G.A. Udourioh, M.M. Solomon, E.I. Epelle, Cell. Mol. Bioeng. (2021) 1–19.
[10] B. Mohan, S. Kumar, V. Kumar, T. Jiao, H.K. Sharma, Q. Chen, TrAC Trends Anal. Chem. 157 (2022) 116735.
[11] N.T.T. Nguyen, T.T.T. Nguyen, S. Ge, R.K. Liew, D.T.C. Nguyen, T. Van Tran, Nanoscale Adv 6 (2024) 1800–1821.
[12] S. Zhang, F. Rong, C. Guo, F. Duan, L. He, M. Wang, Z. Zhang, M. Kang, M. Du, Coord. Chem. Rev. 439 (2021) 213948.
[13] W. Xu, L. Jiao, Y. Wu, L. Hu, W. Gu, C. Zhu, Adv. Mater. 33 (2021) 2005172.
[14] J. Li, H. Jia, X. Ren, Y. Li, L. Liu, R. Feng, H. Ma, Q. Wei, Small 18 (2022) 2106567.
[15] Z. Jin, X. Zhu, N. Wang, Y. Li, H. Ju, J. Lei, Angew. Chem. 132 (2020) 10532–10536.
[16] J. Li, M. Xi, L. Hu, H. Sun, C. Zhu, W. Gu, Anal. Chem. 96 (5) (2024) 2100–2106.

[17] R. Luo, D. Zhu, H. Ju, J. Lei, Acc. Chem. Res. 56 (2023) 1920–1930.
[18] F. Du, Y. Chen, C. Meng, B. Lou, W. Zhang, G. Xu, Curr. Opin. Electrochem. 28 (2021) 100725.
[19] T. Han, Y. Cao, J. Wang, J. Jiao, Y. Song, L. Wang, C. Ma, H.Y. Chen, J.J. Zhu, Adv. Funct. Mater. 33 (2023) 2212394.
[20] H. Wang, L. Liao, Y. Chai, R. Yuan, Biosens. Bioelectron. 150 (2020) 111915.
[21] X. Zhang, C. Li, W. Chen, G. Wang, H. Zou, H. Liu, Front. Chem. 10 (2023) 1106791.
[22] W. Lai, J. Li, M. Jiang, P. Li, M. Wang, C. Ma, C. Zhao, Y. Qi, C. Hong, Anal. Chem. 95 (2023) 7109–7117.
[23] Y. Huang, Z. Wang, Z. Chen, Q. Zhang, Angew. Chem. Int. Ed. 58 (2019) 9696–9711.
[24] Y. Chen, X. Min, X. Zhang, F. Zhang, S. Lu, L.-P. Xu, X. Lou, F. Xia, X. Zhang, S. Wang, Biosens. Bioelectron. 111 (2018) 124–130.
[25] Y. Jia, Anal. Chem. (Washington) 95 (2023) 6725–6731.
[26] H. Peng, Z. Huang, H. Deng, W. Wu, K. Huang, Z. Li, W. Chen, J. Liu, Angew. Chem. Int. Ed. 59 (2020) 9982–9985.
[27] Y. Jia, Y. Du, Z. Ru, D. Fan, L. Yang, X. Ren, Q. Wei, Anal. Chem. 95 (2023) 6725–6731.
[28] X. Lv, Y. Li, B. Cui, Y. Fang, L. Wang, Analyst 147 (2022) 2338–2354.
[29] B. Zhang, Y. Kong, H. Liu, B. Chen, B. Zhao, Y. Luo, L. Chen, Y. Zhang, D. Han, Z. Zhao, Chem. Sci. 12 (2021) 13283–13291.
[30] Z. Wang, M. Xu, N. Zhang, J.-B. Pan, X. Wu, P. Liu, J.-J. Xu, D. Hua, J. Mater. Chem. A 9 (2021) 12584–12592.
[31] Y. Wang, J. Liu, Y. Niu, L. He, Y. Wang, Y. Ma, Y. Yao, J. Ye, Adv. Opt. Mater. 11 (2023) 2202940.
[32] Y. Jia, X. Ren, X. Zhang, D. Wu, H. Ma, Y. Li, Q. Wei, Anal. Chem. 95 (2023) 9139–9144.
[33] J. Tong, Y. Cao, Y.W. Zhang, P. Wang, P. Wang, X.J. Liao, W. Zhang, Y. Wang, Y. X. Zheng, J.J. Zhu, Angew. Chem. 134 (2022) e202209438.
[34] Y. Cao, J.-L. Zhou, Y. Ma, Y. Zhou, J.-J. Zhu, Dalton Trans. 51 (2022) 8927–8937.
[35] Y. Jia, M. Zhu, X. Zhang, D. Jia, T. Tian, B. Shi, Z. Ru, H. Ma, Y. Wan, Q. Wei, Anal. Chem. 96 (2024) 10116–10120.
[36] J. Mei, Y. Hong, J.W.Y. Lam, A. Qin, Y. Tang, B.Z. Tang, Adv. Mater. 26 (2014) 5429–5479.
[37] W. Guo, L. Zhao, L. Jiang, Y. Nie, Y. Zhou, TrAC Trends Anal. Chem. 170 (2023) 117443.
[38] Z. Qiao, R. Jiang, H. Xu, D. Cao, X.C. Zeng, Angew. Chem. (2024) e202407812.
[39] W. Wei, H. Ze, Z. Qiu, TrAC Trends Anal. Chem. 161 (2023) 116997.
[40] Y. Zhang, Y. Chen, Y. Nie, Z. Yang, R. Yuan, H. Wang, Y. Chai, Anal. Chem. 94 (2022) 12196–12203.
[41] C. Hu, L. Cao, X. Wu, G. Chen, Y. Li, J. Wang, C. Huang, L. Zhan, Biosens. Bioelectron. 255 (2024) 116263.
[42] Y. Han, Z. Gao, C. Wang, R. Zhong, F. Wang, Coord. Chem. Rev. 414 (2020) 213300.
[43] M.H. Chua, B.Y.K. Hui, K.L.O. Chin, Q. Zhu, X. Liu, J. Xu, Mater. Chem. Front. 7 (2023) 5561–5660.
[44] L. Yang, J. Li, Chemosensors 11 (2023) 432.
[45] I. Nandi, S. Rai, P. Chandra, Talanta 266 (2023) 125124.
[46] X. Lv, M. Bi, X. Xu, Y. Li, C. Geng, B. Cui, Y. Fang, Anal. Bioanal. Chem. 414 (2022) 1389–1402.
[47] G. Sun, Y. Xie, L. Sun, H. Zhang, Nanoscale Horizons 6 (2021) 766–780.
[48] Y.-P. Huo, S. Liu, Z.-X. Gao, B.-A. Ning, Y. Wang, Microchim. Acta 188 (2021) 1–29.
[49] U. Chadha, P. Bhardwaj, R. Agarwal, P. Rawat, R. Agarwal, I. Gupta, M. Panjwani, S. Singh, C. Ahuja, S.K. Selvaraj, J. Ind. Eng. Chem. 109 (2022) 21–51.
[50] X. Liu, H. Cheng, Y. Zhao, Y. Wang, F. Li, Biosens. Bioelectron. 199 (2022) 113906.
[51] T.-Y. Luo, P. Das, D.L. White, C. Liu, A. Star, N.L. Rosi, J. Am. Chem. Soc. 142 (2020) 2897–2904.
[52] P. Liu, X. Li, X. Xu, K. Ye, L. Wang, H. Zhu, M. Wang, X. Niu, Sensors Actuators B Chem. 328 (2021) 129024.
[53] S. Hu, J. Liu, Y. Wang, Z. Liang, B. Hu, J. Xie, W.-L. Wong, K.-Y. Wong, B. Qiu, W. Peng, Sensors Actuators B Chem. 380 (2023) 133379.
[54] J. Xu, R. Li, Z. Xu, X. Chen, Y. Li, T. Zhao, L. Jia, Sensors Actuators B Chem. 369 (2022) 132341.
[55] L. Zhao, X. Song, X. Ren, D. Fan, Q. Wei, D. Wu, Anal. Chem. 93 (2021) 8613–8621.
[56] S.A. Younis, N. Bhardwaj, S.K. Bhardwaj, K.-H. Kim, A. Deep, Coord. Chem. Rev. 429 (2021) 213620.
[57] S. Dong, L. Peng, W. Wei, T. Huang, ACS Appl. Mater. Interfaces 10 (2018) 14665–14672.
[58] J.-M. Wang, X. Lian, B. Yan, Inorg. Chem. 58 (2019) 9956–9963.
[59] L. Zhao, Biosens. Bioelectron. 191 (2021).
[60] M. Yuan, J. Chem. Educ. 96 (2019) 1256–1261.
[61] H.-Q. Yin, J. Am. Chem. Soc. 141 (2019) 15166–15173.
[62] Y. Zhao, J. Mater. Chem. C, Mater. Opt. Electronic Dev. 8 (2020) 12739–12754.
[63] K. Wu, Inorg. Chem. Front. 9 (2022) 1714–1721.
[64] Y. Wang, J. Liu, Y. Niu, L. He, Y. Wang, Y. Ma, Y. Yao, J. Ye, Adv. Opt. Mater. 11 (2023) 2202940.
[65] J. Yang, D. Qin, N. Wang, Y. Wu, K. Fang, B. Deng, Anal. Chem. 95 (2023) 7045–7052.
[66] L. Ma, D. Wu, L. Hu, R. Xiao, K. Pei, W. Qi, Sensors Actuators B Chem. 407 (2024) 135460.
[67] J. Li, M. Luo, C. Jin, P. Zhang, H. Yang, R. Cai, W. Tan, ACS Appl. Mater. Interfaces 14 (2022) 383–389.
[68] Y. Jia, Anal. Chem. (Washington) 95 (2023) 9139–9144.
[69] Y. Jia, Anal. Chem. (Washington) 96 (2024) 10116–10120.
[70] X. Jiang, H. Jin, Y. Sun, Z. Sun, R. Gui, Biosens. Bioelectron. 152 (2020) 112012.
[71] J. Ma, W. Bai, J. Zheng, Microchim. Acta 186 (2019) 482.
[72] P.-P. Dong, Y.-Y. Liu, Q.-C. Peng, H.-Y. Li, K. Li, S.-Q. Zang, B.Z. Tang, Dalton Trans. 52 (2023) 1913–1918.
[73] X. Zhai, Y. Kou, L. Liang, P. Liang, P. Su, Y. Tang, Inorg. Chem. 62 (2023) 18533–18542.
[74] T. Mehmood, J.P. Reddy, Chapter seven - AIE-MOF materials for biological applications, in: R.S. Bhosale, V. Singh (Eds.), Progress in Molecular Biology and Translational Science, Academic Press, 2021, pp. 179–198.
[75] Y. Zhao, J. Wang, W. Zhu, L. Liu, R. Pei, Nanoscale 13 (2021) 4505–4511.
[76] L. Zhu, B. Zhu, J. Luo, B. Liu, ACS Mater. Lett. 3 (2021) 77–89.
[77] M. Asad, M. Imran Anwar, A. Abbas, A. Younas, S. Hussain, R. Gao, L.-K. Li, M. Shahid, S. Khan, Coord. Chem. Rev. 463 (2022) 214539.
[78] A.E. Thorarinsdottir, T.D. Harris, Chem. Rev. 120 (2020) 8716–8789.
[79] L. Feng, K.-Y. Wang, J. Willman, H.-C. Zhou, ACS Cent. Sci. 6 (2020) 359–367.
[80] M. Shen, H. Ma, Coord. Chem. Rev. 470 (2022) 214715.
[81] W. Fan, X. Zhang, Z. Kang, X. Liu, D. Sun, Coord. Chem. Rev. 443 (2021) 213968.
[82] H.-Y. Li, S.-N. Zhao, S.-Q. Zang, J. Li, Chem. Soc. Rev. 49 (2020) 6364–6401.
[83] R.F. Mendes, F. Figueira, J.P. Leite, L. Gales, F.A.A. Paz, Chem. Soc. Rev. 49 (2020) 9121–9153.
[84] X. Fu, B. Ding, D. D'Alessandro, Coord. Chem. Rev. 475 (2023) 214814.
[85] M.T. Ulhakim, M. Rezki, K.K. Dewi, S.A. Abrori, S. Harimurti, N.L.W. Septiani, K. A. Kurnia, W. Setyaningsih, N. Darmawan, B. Yuliarto, J. Electrochem. Soc. 167 (2020) 136509.
[86] J. Zhou, Y. Li, W. Wang, X. Tan, Z. Lu, H. Han, Biosens. Bioelectron. 164 (2020) 112332.
[87] P. Li, L. Luo, D. Cheng, Y. Sun, Y. Zhang, M. Liu, S. Yao, Anal. Chem. 94 (2022) 5707–5714.
[88] X. Ren, M. Shao, X. Li, Z. Xie, J. Zhao, H. Wang, M. Gao, D. Wu, H. Ju, Q. Wei, Talanta 273 (2024) 125959.
[89] M. Yan, J. Ye, Q. Zhu, L. Zhu, J. Huang, X. Yang, Anal. Chem. 91 (2019) 10156–10163.
[90] Y. Wang, Y. Li, X. Zhuang, C. Tian, X. Fu, F. Luan, Biosens. Bioelectron. 190 (2021) 113371.
[91] H. Dong, S. Liu, Q. Liu, Y. Li, Z. Xu, Y. Li, Q. Wei, Anal. Chem. 94 (2022) 12852–12859.
[92] Y. Ding, X. Zhang, J. Peng, D. Zheng, X. Zhang, Y. Song, Y. Chen, W. Gao, Sensors Actuators B Chem. 324 (2020) 128700.
[93] Y. Li, M. Karimi, Y.-N. Gong, N. Dai, V. Safarifard, H.-L. Jiang, Matter 4 (2021) 2230–2265.
[94] S. Haddad, I. Abánades Lázaro, M. Fantham, A. Mishra, J. Silvestre-Albero, J. W. Osterrieth, G.S. Kaminski Schierle, C.F. Kaminski, R.S. Forgan, D. Fairen-Jimenez, J. Am. Chem. Soc. 142 (2020) 6661–6674.
[95] Q. Zeng, X. Li, W. Gong, S. Guo, Y. Ouyang, D. Li, Y. Xiao, C. Tan, L. Xie, H. Lu, Adv. Energy Mater. 12 (2022) 2104074.
[96] H. Lyu, O.I.-F. Chen, N. Hanikel, M.I. Hossain, R.W. Flaig, X. Pei, A. Amin, M. D. Doherty, R.K. Impastato, T.G. Glover, J. Am. Chem. Soc. 144 (2022) 2387–2396.
[97] X. Li, W. Ma, H. Li, Q. Zhang, H. Liu, Coord. Chem. Rev. 408 (2020) 213191.
[98] M. Lv, W. Zhou, H. Tavakoli, C. Bautista, J. Xia, Z. Wang, X. Li, Biosens. Bioelectron. 176 (2021) 112947.
[99] S.H. Paiman, M.A. Rahman, T. Uchikoshi, N. Abdullah, M.H.D. Othman, J. Jaafar, K.H. Abas, A.F. Ismail, J. Saudi Chem. Soc. 24 (2020) 896–905.
[100] I. Ahmed, M.M.H. Mondol, M.J. Jung, G.H. Lee, S.H. Jhung, Coord. Chem. Rev. 475 (2023) 214912.
[101] B. Liu, M. Jiang, D. Zhu, J. Zhang, G. Wei, Chem. Eng. J. 428 (2022) 131118.
[102] K. Song, X. Su, W. Zhao, F. Ai, A. Umar, S. Baskoutas, Chem. Eng. J. 485 (2024) 150067.
[103] S. Ali Akbar Razavi, A. Morsali, Coord. Chem. Rev. 399 (2019) 213023.
[104] S. Fajal, P. Samanta, S. Dutta, S.K. Ghosh, Inorg. Chim. Acta 502 (2020) 119359.
[105] L. Feng, G.S. Day, K.-Y. Wang, S. Yuan, H.-C. Zhou, Chem 6 (2020) 2902–2923.
[106] Q.-Q. Zhu, Q.-S. Zhou, H.-W. Zhang, W.-W. Zhang, D.-Q. Lu, M.-T. Guo, Y. Yuan, F. Sun, H. He, Inorg. Chem. 59 (2020) 1323–1331.
[107] X. Gong, K. Gnanasekaran, Z. Chen, L. Robison, M.C. Wasson, K.C. Bentz, S. M. Cohen, O.K. Farha, N.C. Gianneschi, J. Am. Chem. Soc. 142 (2020) 17224–17235.
[108] T.C. Narayan, T. Miyakai, S. Seki, M. Dincă, J. Am. Chem. Soc. 134 (2012) 12932–12935.
[109] J.-S. Qin, S. Yuan, L. Zhang, B. Li, D.-Y. Du, N. Huang, W. Guan, H.F. Drake, J. Pang, Y.-Q. Lan, J. Am. Chem. Soc. 141 (2019) 2054–2060.
[110] P. Pashazadeh-Panahi, S. Belali, H. Sohrabi, F. Oroojalian, M. Hashemzaei, A. Mokhtarzadeh, M. de la Guardia, TrAC Trends Anal. Chem. 141 (2021) 116285.
[111] S. Dutta, J. Kim, P.H. Hsieh, Y.S. Hsu, Y.V. Kaneti, F.K. Shieh, Y. Yamauchi, K.C. W. Wu, Small Methods 3 (2019) 1900213.
[112] W. Duan, Z. Zhao, H. An, Z. Zhang, P. Cheng, Y. Chen, H. Huang, Met.-Organic Framework: From Des. Appl. (2020) 57–87.
[113] H. An, M. Li, J. Gao, Z. Zhang, S. Ma, Y. Chen, Coord. Chem. Rev. 384 (2019) 90–106.
[114] Z. Sharifzadeh, A. Morsali, Coord. Chem. Rev. 459 (2022) 214445.
[115] W. Ma, H. Lu, B. Yan, J. Colloid Interface Sci. 601 (2021) 427–436.
[116] A. Shahzaib, L.A. Kamran, N. Nishat, Mater. Today Chem. 34 (2023) 101781.

[117] J.S. Kahn, L. Freage, N. Enkin, M. Garcia, I. Willner, Adv. Mater. (Deerfield Beach, Fla.) 29 (2016).
[118] D. Zhu, Y. Zhang, S. Bao, N. Wang, S. Yu, R. Luo, J. Ma, H. Ju, J. Lei, J. Am. Chem. Soc. 143 (2021) 3049–3053.
[119] S. He, Q. Liu, Y. Ji, P. Zhang, C. Huang, J. Sun, Y. Lu, D.-P. Yang, N. Jia, J. Mater. Chem. B 10 (2022) 7789–7796.
[120] L. Li, B. Chen, L. Luo, X. Liu, X. Bi, T. You, Talanta 222 (2021) 121579.
[121] X. Xu, X. Qin, L. Wang, X. Wang, J. Lu, X. Qiu, Y. Zhu, Analyst 144 (2019) 2359–2366.
[122] C. Bashore, S. Prakash, M.C. Johnson, R.J. Conrad, I.A. Kekessie, S.J. Scales, N. Ishisoko, T. Kleinheinz, P.S. Liu, N. Popovych, Nat. Chem. Biol. 19 (2023) 55–63.
[123] J. Wu, A. Wang, P. Liu, Y. Hou, L. Song, R. Yuan, Y. Fu, Sensors Actuators B Chem. 321 (2020) 128531.
[124] M. Zhang, M. Qian, H. Huang, Q. Gao, C. Zhang, H. Qi, J. Electroanal. Chem. 920 (2022) 116578.
[125] X. Zhang, P. Wang, Y. Nie, Q. Ma, TrAC Trends Anal. Chem. 143 (2021) 116410.
[126] D. Han, B. Goudeau, D. Manojlovic, D. Jiang, D. Fang, N. Sojic, Angew. Chem. 133 (2021) 7764–7768.
[127] H. Cheng, P. Hui, J. Peng, W. Li, W. Ma, H. Wang, J. Huang, X. He, K. Wang, Anal. Chem. 93 (2021) 6770–6778.
[128] Z. Wei, H. Zhang, F. Zhang, J. Xia, Q. Meng, H. Huang, Z. Wang, Biosens. Bioelectron. 256 (2024) 116236.
[129] Y. Zhao, D. Li, J. Mater. Chem. C 8 (2020) 12739–12754.
[130] Y. Zhao, N. Zhang, Y. Wang, F.Y. Bai, Y.H. Xing, L.X. Sun, Inorg. Chem. Front. 8 (2021) 1736–1746.
[131] M.H. Lee, N. Park, C. Yi, J.H. Han, J.H. Hong, K.P. Kim, D.H. Kang, J.L. Sessler, C. Kang, J.S. Kim, J. Am. Chem. Soc. 136 (2014) 14136–14142.
[132] S.V. Eliseeva, J.-C.G. Bünzli, Chem. Soc. Rev. 39 (2010) 189–227.
[133] F. Chen, Y.-M. Wang, W. Guo, X.-B. Yin, Chem. Sci. 10 (2019) 1644–1650.
[134] Y. Peng, S. Sanati, A. Morsali, H. García, Angew. Chem. Int. Ed. 62 (2023) e202214707.
[135] Y. Zhang, X. Zheng, X. Guo, J. Zhang, A. Yuan, Y. Du, F. Gao, Appl. Catal. B Environ. 336 (2023) 122891.
[136] C.P. Wang, H.Y. Liu, G. Bian, X. Gao, S. Zhao, Y. Kang, J. Zhu, X.H. Bu, Small 15 (2019) 1906086.
[137] S. Zhao, Y. Wang, J. Dong, C.-T. He, H. Yin, P. An, K. Zhao, X. Zhang, C. Gao, L. Zhang, Nat. Energy 1 (2016) 1–10.
[138] W. Cheng, X.F. Lu, D. Luan, X.W. Lou, Angew. Chem. Int. Ed. 59 (2020) 18234–18239.
[139] J. Yang, Y.W. Yang, Small 16 (2020) 1906846.
[140] M. Mozafari, Metal-Organic Frameworks for Biomedical Applications, Woodhead Publishing, 2020.
[141] B. Yang, L. Ding, H. Yao, Y. Chen, J. Shi, Adv. Mater. 32 (2020) 1907152.
[142] P. Chen, Z. Liu, J. Liu, H. Liu, W. Bian, D. Tian, F. Xia, C. Zhou, Electrochim. Acta 354 (2020) 136644.
[143] C. Wang, Z. Li, H. Ju, Anal. Chem. 93 (2021) 14878–14884.
[144] C. Dai, Y. Gan, J. Qin, L. Ma, Q. Liu, L. Huang, Z. Yang, G. Zang, S. Zhu, Colloids Surf. B: Biointerfaces. 226 (2023) 113322.
[145] L. Zheng, Q. Guo, C. Yang, J. Wang, X. Xu, G. Nie, Sensors Actuators B Chem. 379 (2023) 133269.
[146] Y. Zhao, Z. Mao, J. Jia, C. Dai, L. Li, Y. Zhou, Anal. Chem. 95 (2023) 17117–17124.
[147] S.-S. Song, J. Zhan, H.-T. Zhu, J.-Y. Bao, A.-J. Wang, P.-X. Yuan, J.-J. Feng, Analyst 149 (2024) 426–434.
[148] B. Wang, L. Zhao, Y. Li, X. Liu, D. Fan, D. Wu, Q. Wei, Anal. Chim. Acta 1276 (2023) 341616.
[149] H.-Q. Yin, X.-B. Yin, Acc. Chem. Res. 53 (2020) 485–495.
[150] M. Gutiérrez, Y. Zhang, J.-C. Tan, Chem. Rev. 122 (2022) 10438–10483.
[151] C.-Y. Liu, X.-R. Chen, H.-X. Chen, Z. Niu, H. Hirao, P. Braunstein, J.-P. Lang, J. Am. Chem. Soc. 142 (2020) 6690–6697.
[152] H.-Q. Yin, J.-C. Yang, X.-B. Yin, Anal. Chem. 89 (2017) 13434–13440.
[153] X. Gao, Y. Wang, G. Ji, R. Cui, Z. Liu, CrystEngComm 20 (2018) 1087–1093.
[154] G. Ji, T. Zheng, X. Gao, Z. Liu, Sensors Actuators B Chem. 284 (2019) 91–95.
[155] Y. Liu, Y. Huo, X. Wang, S. Yu, Y. Ai, Z. Chen, P. Zhang, L. Chen, G. Song, N. S. Alharbi, J. Clean. Prod. 278 (2021) 123216.
[156] G. Chen, S. Huang, X. Kou, F. Zhu, G. Ouyang, Angew. Chem. 132 (2020) 14051–14058.
[157] L.B. Vaidya, S.S. Nadar, V.K. Rathod, Colloids Surf. B: Biointerfaces 193 (2020) 111052.
[158] G. Chen, S. Huang, X. Kou, S. Wei, S. Huang, S. Jiang, J. Shen, F. Zhu, G. Ouyang, Angew. Chem. Int. Ed. 58 (2019) 1463–1467.
[159] N. Zhong, R. Gao, Y. Shen, X. Kou, J. Wu, S. Huang, G. Chen, G. Ouyang, Anal. Chem. 94 (2022) 14385–14393.
[160] W.-H. Li, W.-H. Deng, G.-E. Wang, G. Xu, EnergyChem 2 (2020) 100029.
[161] L.S. Xie, G. Skorupskii, M. Dinca, Chem. Rev. 120 (2020) 8536–8580.
[162] C. Wu, P. Geng, G. Zhang, X. Li, H. Pang, Small 20 (2024) 2308264.
[163] J.-L. Zhang, S. Gao, Y. Yang, W.-B. Liang, M.-L. Lu, X.-Y. Zhang, H.-X. Xiao, Y. Li, R. Yuan, D.-R. Xiao, Biosens. Bioelectron. 227 (2023) 115157.
[164] C. Xiong, J. Huang, H. Liu, M.-M. Chen, W. Wen, X. Zhang, S. Wang, Talanta 249 (2022) 123602.
[165] L.-Y. Huang, X. Hu, H.-Y. Shan, L. Yu, Y.-X. Gu, A.-J. Wang, D. Shan, P.-X. Yuan, J.-J. Feng, Sensors Actuators B Chem. 344 (2021) 130300.
[166] X. Lv, X. Xu, T. Miao, X. Zang, C. Geng, Y. Li, B. Cui, Y. Fang, Sensors Actuators B Chem. 352 (2022) 131026.
[167] T. Tang, F. Yang, L. Wang, C. Zhao, F. Nie, Guoping Yang, Microchim. Acta 187 (2020) 1–11.
[168] C. Li, T. Hang, Y. Jin, Exploration, Wiley Online Library, 2023, pp. 20220151.
[169] W. Zhong, Y. Zhang, H. Zhao, Z. Liang, J. Shi, Q. Ma, Talanta 265 (2023) 124875.
[170] S. Wang, M. Wang, C. Li, H. Li, C. Ge, X. Zhang, Y. Jin, Sensors Actuators B Chem. 311 (2020) 127919.
[171] D. Bahari, B. Babamiri, K. Moradi, A. Salimi, R. Hallaj, Biosens. Bioelectron. 195 (2022) 113657.
[172] X.-H. Wei, X. Qiao, J. Fan, Y.-Q. Hao, Y.-T. Zhang, Y.-L. Zhou, M.-T. Xu, Microchem. J. 173 (2022) 106910.
[173] H. Sun, Z. Li, Y. Gu, C. Guo, Chin. J. Struct. Chem. 41 (2022) 2211018–2211030.
[174] B.B. Guo, J.C. Yin, N. Li, Z.X. Fu, X. Han, J. Xu, X.H. Bu, Adv. Opt. Mater. 9 (2021) 2100283.
[175] E.A. Dolgopolova, A.A. Berseneva, M.S. Faillace, O.A. Ejegbavwo, G.A. Leith, S. W. Choi, H.N. Gregory, A.M. Rice, M.D. Smith, M. Chruszcz, J. Am. Chem. Soc. 142 (2020) 4769–4783.
[176] X. Xiong, C. Xiong, Y. Gao, Y. Xiao, M.-M. Chen, W. Wen, X. Zhang, S. Wang, Anal. Chem. 94 (2022) 7861–7867.
[177] J. Fang, L. Dai, R. Feng, W. Cao, X. Ren, X. Li, D. Wu, Q. Wei, H. Ma, J. Colloid Interface Sci. 665 (2024) 934–943.
[178] L. Zhao, X. Ren, H. Ma, H. Wang, Y. Li, Q. Wei, D. Wu, H. Ju, Anal. Chem. 95 (2023) 13463–13469.
[179] L. Kong, M. Zhong, W. Shuang, Y. Xu, X.-H. Bu, Chem. Soc. Rev. 49 (2020) 2378–2407.
[180] E. Cossar, M.S. Houache, Z. Zhang, E.A. Baranova, J. Electroanal. Chem. 870 (2020) 114246.
[181] R. Du, Y. Wu, Y. Yang, T. Zhai, T. Zhou, Q. Shang, L. Zhu, C. Shang, Z. Guo, Adv. Energy Mater. 11 (2021) 2100154.
[182] S. Li, Y. Gao, N. Li, L. Ge, X. Bu, P. Feng, Energy Environ. Sci. 14 (2021) 1897–1927.
[183] T.-Z. Liu, R. Hu, X. Zhang, K.-L. Zhang, Y. Liu, X.-B. Zhang, R.-Y. Bai, D. Li, Y.-H. Yang, Anal. Chem. 88 (2016) 12516–12523.
[184] R. Hu, X. Zhang, K.-N. Chi, T. Yang, Y.-H. Yang, ACS Appl. Mater. Interfaces 12 (2020) 30770–30778.
[185] X. Yang, J. Lv, Z. Yang, R. Yuan, Y. Chai, Anal. Chem. 89 (2017) 11636–11640.
[186] X. Tan, S. Wang, N. Han, Chemosphere 313 (2023) 137330.
[187] B. Ding, M.B. Solomon, C.F. Leong, D.M. D'Alessandro, Coord. Chem. Rev. 439 (2021) 213891.
[188] J. Calbo, M.J. Golomb, A. Walsh, J. Mater. Chem. A 7 (2019) 16571–16597.
[189] J. Li, H. Yang, R. Cai, W. Tan, Anal. Chem. 96 (27) (2024) 11076–11082.
[190] H. Wu, M. Li, Z. Wang, H. Yu, J. Han, G. Xie, S. Chen, Anal. Chim. Acta 1049 (2019) 74–81.
[191] C.-M. Ngue, M.-K. Leung, K.-L. Lu, Inorg. Chem. 59 (2020) 2997–3003.
[192] C.-M. Ngue, Y.-H. Liu, M.-K. Leung, K.-L. Lu, Inorg. Chem. 60 (2021) 11458–11465.
[193] G. Zhao, X. Dong, Y. Du, N. Zhang, G. Bai, D. Wu, H. Ma, Y. Wang, W. Cao, Q. Wei, Anal. Chem. 94 (2022) 10557–10566.
[194] C. Su, Q. Song, D. Jiang, C. Dong, X. Shan, Z. Chen, Analyst 146 (2021) 4254–4260.
[195] Y.-Q. Xue, N. Liao, Y. Li, W.-B. Liang, X. Yang, X. Zhong, Y. Zhuo, Biosens. Bioelectron. 217 (2022) 114713.
[196] Z. Dourandish, S. Tajik, H. Beitollahi, P.M. Jahani, F.G. Nejad, I. Sheikhshoaie, A. Di Bartolomeo, Sensors 22 (2022) 2238.
[197] S. Liu, C. Lai, X. Liu, B. Li, C. Zhang, L. Qin, D. Huang, H. Yi, M. Zhang, L. Li, Coord. Chem. Rev. 424 (2020) 213520.
[198] X. Xiong, Y. Zhang, Y. Wang, H. Sha, N. Jia, Sensors Actuators B Chem. 297 (2019) 126812.
[199] F. Yang, W. Wang, M. Zhang, W. Tao, Y. Wang, J. Shi, Y. Ding, M. Xie, S. Zhang, Z. Fan, Environ. Sci. Nano 9 (2022) 3417–3426.
[200] D. Feng, P. Li, X. Tan, Y. Wu, F. Wei, F. Du, C. Ai, Y. Luo, Q. Chen, H. Han, Anal. Chim. Acta 1100 (2020) 232–239.
[201] W. Zhang, L. Chen, K. Yang, L. Wang, B. Han, S. Sun, J. Wen, Sensors Actuators B Chem. 393 (2023) 134317.
[202] L. Yang, S. Zhang, X. Liu, Y. Tang, Y. Zhou, D.K. Wong, J. Mater. Chem. B 8 (2020) 7880–7893.
[203] C. Zhou, H. Zou, C. Sun, Y. Li, Food Chem. 361 (2021) 130109.
[204] L. Bezinge, A. Suea-Ngam, A.J. deMello, C.-J. Shih, Mol. Syst. Des. Eng. 5 (2020) 49–66.
[205] M. Zhao, K. Yuan, Y. Wang, G. Li, J. Guo, L. Gu, W. Hu, H. Zhao, Z. Tang, Nature 539 (2016) 76–80.
[206] N. Huang, S. Yuan, H. Drake, X. Yang, J. Pang, J. Qin, J. Li, Y. Zhang, Q. Wang, D. Jiang, J. Am. Chem. Soc. 139 (2017) 18590–18597.
[207] Y. Ren, M. Shi, W. Zhang, D.D. Dionysiou, J. Lu, C. Shan, Y. Zhang, L. Lv, B. Pan, Environ. Sci. Technol. 54 (2020) 5258–5267.
[208] Y. Ma, M. Li, J. Jiang, T. Li, X. Wang, Y. Song, S. Dong, J. Alloys Compd. 870 (2021) 159524.
[209] X. Han, N. Wang, W. Zhang, X. Liu, Q. Yu, J. Lei, L. Zhou, G. Xiu, J. Environ. Chem. Eng. 11 (2023) 109144.
[210] R. El Asmar, A. Baalbaki, Z. Abou Khalil, S. Naim, A. Bejjani, A. Ghauch, Chem. Eng. J. 405 (2021) 126701.
[211] Y. Hu, Z. Zhong, M. Lu, Y. Muhammad, S.J. Shah, H. He, W. Gong, Y. Ren, X. Yu, Z. Zhao, Chem. Eng. J. 450 (2022) 137964.
[212] Y. Xie, C. Liu, D. Li, Y. Liu, Appl. Surf. Sci. 592 (2022) 153312.
[213] X. Wang, C. Yang, S. Zhu, M. Yan, S. Ge, J. Yu, Biosens. Bioelectron. 87 (2017) 108–115.

[214] W.-J. Shen, Y. Zhuo, Y.-Q. Chai, R. Yuan, Biosens. Bioelectron. 83 (2016) 287–292.
[215] P. Ling, J. Lei, H. Ju, Anal. Chem. 88 (2016) 10680–10686.
[216] H. Cheng, Y. Liu, Y. Hu, Y. Ding, S. Lin, W. Cao, Q. Wang, J. Wu, F. Muhammad, X. Zhao, Anal. Chem. 89 (2017) 11552–11559.
[217] H. Liu, Z. Liu, J. Yi, D. Ma, F. Xia, D. Tian, C. Zhou, Sensors Actuators B Chem. 331 (2021) 129412.
[218] G. Zhao, Y. Wang, X. Li, Q. Yue, X. Dong, B. Du, W. Cao, Q. Wei, Anal. Chem. 91 (2019) 1989–1996.
[219] X. Song, S. Yu, L. Zhao, Y. Guo, X. Ren, H. Ma, S. Wang, C. Luo, Y. Li, Q. Wei, Anal. Chem. 94 (2022) 9363–9371.
[220] X. Cheng, X. Zhou, Z. Zheng, Q. Kuang, Chem. Eng. J. 430 (2022) 133079.
[221] C. Chen, J. Li, Z. Lv, M. Wang, J. Dang, Int. J. Hydrog. Energy 48 (78) (2023) 30435–30463.
[222] H. Yu, J. Han, S. An, G. Xie, S. Chen, Biosens. Bioelectron. 109 (2018) 63–69.
[223] S. Yuan, R. Yu, Y. Tu, Y. Du, X. Feng, F. Nie, Talanta 254 (2023) 124183.
[224] L. Zheng, Q. Li, X. Deng, Q. Guo, D. Liu, G. Nie, J. Colloid Interface Sci. 659 (2024) 859–867.
[225] H. Yang, J. Liu, X. Feng, F. Nie, G. Yang, Anal. Bioanal. Chem. 413 (2021) 4407–4416.
[226] X. Shan, T. Pan, Y. Pan, W. Wang, X. Chen, X. Shan, Z. Chen, Electroanalysis 32 (2020) 462–469.
[227] Y. Jiao, S. Cheng, F. Wu, X. Pan, A. Xie, X. Zhu, W. Dong, Compos. Part B Eng. 211 (2021) 108643.
[228] K.I. Hadjiivanov, D.A. Panayotov, M.Y. Mihaylov, E.Z. Ivanova, K.K. Chakarova, S.M. Andonova, N.L. Drenchev, Chem. Rev. 121 (2021) 1286–1424.
[229] X.T. Liu, B.B. Qian, D.S. Zhang, M.H. Yu, Z. Chang, X.H. Bu, Coord. Chem. Rev. 476 (2023) 214921.
[230] L. Zhao, X. Song, X. Ren, H. Wang, D. Fan, D. Wu, Q. Wei, Biosens. Bioelectron. 191 (2021) 113409.
[231] Q. Wang, X. Zhang, L. Huang, Z. Zhang, S. Dong, Angew. Chem. Int. Ed. 56 (2017) 16082–16085.
[232] X. Lian, Y.-P. Chen, T.-F. Liu, H.-C. Zhou, Chem. Sci. 7 (2016) 6969–6973.
[233] J.A. Cruz-Navarro, F. Hernandez-Garcia, G.A. Alvarez Romero, Coord. Chem. Rev. 412 (2020) 213263.
[234] M. Rezki, N.L.W. Septiani, M. Iqbal, S. Harimurti, P. Sambegoro, D.R. Adhika, B. Yuliarto, J. Mater. Chem. B 9 (2021) 5711–5721.
[235] J. Chang, W. Lv, Q. Li, H. Li, F. Li, Anal. Chem. 92 (2020) 8959–8964.
[236] T. Bao, R. Fu, W. Wen, X. Zhang, S. Wang, ACS Appl. Mater. Interfaces 12 (2020) 2087–2094.
[237] L. Chen, N. Tsumori, Q. Xu, Sci. China Chem. 63 (2020) 1601–1607.
[238] N. Ye, X. Kou, J. Shen, S. Huang, G. Chen, G. Ouyang, ChemBioChem 21 (2020) 2585–2590.
[239] L. Dai, Y. Li, Y. Wang, X. Luo, D. Wei, R. Feng, T. Yan, X. Ren, B. Du, Q. Wei, Biosens. Bioelectron. 132 (2019) 97–104.
[240] C. Gu, C. Guo, Z. Li, M. Wang, N. Zhou, L. He, Z. Zhang, M. Du, Biosens. Bioelectron. 134 (2019) 8–15.
[241] H. Yu, W. Zhang, S. Lv, J. Han, G. Xie, S. Chen, Chem. Commun. 54 (2018) 11901–11904.
[242] S. Wang, M. Wang, C. Li, H. Li, C. Ge, X. Zhang, Y. Jin, Sensors Actuators B Chem. 311 (2020) 127919.
[243] W. Wu, Y. Li, P. Song, Q. Xu, N. Long, P. Li, L. Zhou, B. Fu, J. Wang, W. Kong, Trends Food Sci. Technol. 138 (2023) 238–271.
[244] B. Liu, M. Sun, T. Li, P. Liang, Q. Zhou, M. Guo, C. Li, W.-J. Duan, M.-M. Li, J.-X. Chen, B.-P. Xie, Z. Dai, J. Chen, Sensors Actuators B Chem. 387 (2023) 133812.
[245] Y. Gao, D. Zhou, Q. Xu, J. Li, W. Luo, J. Yang, Y. Pan, T. Huang, Y. Wang, B. He, Y. Song, Y. Wang, ACS Appl. Mater. Interfaces 15 (2023) 5010–5018.
[246] Y. Zhao, J. Chen, H. Zhong, C. Zhang, Y. Zhou, W. Mao, C. Yu, Microchim. Acta 187 (2020) 649.
[247] Z. Sun, L. Wang, S. Wu, Y. Pan, Y. Dong, S. Zhu, J. Yang, Y. Yin, G. Li, Anal. Chem. 92 (2020) 3819–3826.
[248] J. Gao, S. Luo, Y. Fan, Y. Ma, L. Wang, Z. Fu, Anal. Chim. Acta 1282 (2023) 341909.
[249] Y.-J. Li, W.-R. Cui, Q.-Q. Jiang, Q. Wu, R.-P. Liang, Q.-X. Luo, J.-D. Qiu, Nat. Commun. 12 (2021) 4735.
[250] J.-L. Zhang, Y. Yang, W.-B. Liang, L.-Y. Yao, R. Yuan, D.-R. Xiao, Anal. Chem. 93 (2021) 3258–3265.
[251] S. Li, X. Zhu, H. Liu, B. Sun, Coord. Chem. Rev. 518 (2024) 216046.
[252] L. Cui, Y. Yang, S. Jiang, X. Cao, W. Chu, J. Chen, B. Sun, K. Ren, C.-Y. Zhang, ACS Sens. 9 (2024) 1023–1030.
[253] W.-J. Zeng, K. Wang, W.-B. Liang, Y.-Q. Chai, R. Yuan, Y. Zhuo, Chem. Sci. 11 (2020) 5410–5414.
[254] Y. Zhou, Z. Mao, J.-J. Xu, Chin. Chem. Lett. 35 (2024) 109622.
[255] M.-L. Lu, W. Huang, S. Gao, J.-L. Zhang, W.-B. Liang, Y. Li, R. Yuan, D.-R. Xiao, Anal. Chem. 94 (2022) 15832–15838.